Quantum Stabilization by Coherent Population of Scarred Eigenstates: Quantum Suppression of Transport Classically Initiated by Separatrix Band Entry

Luca C. Perotti
Department of Physics, Texas Southern University, Houston, Texas 77004 USA
(Dated: June 29, 2009)

Comparisons of experimental data with numerical predictions of a classical model indicate that an excited hydrogen atom in a pulsed microwave electric field exhibits a nonclassical increase of stability over a relatively wide range of frequencies. I show here that this is due to selective population of long-lived "scarred" states that are associated with the chaotic separatrix band surrounding the principal classical resonance zone in phase space. A quantum explanation is given in terms of adiabatic evolution of Floquet states and the destabilizing effect of two-level quantum resonances is investigated. The role of neighbouring classical resonance zones in defining the frequency range of stabilization is revealed both by quasienergy curves and by Husimi functions for the instantaneous quantum states.

PACS numbers: 05.45.Mt, 03.65.-w, 32.80.Rm, 47.20.Ky

I. INTRODUCTION

Since early in the development of quantum mechanics, it has been apparent the importance of coherent wavepackets as "semiclassical" objects following a classical orbit in phase space [1, 2]. In most systems this semiclassical behaviour is relatively short lived, as the packets have to be built as a superposition of eigenstates of the system [3] and dephasing soon breaks them up. "Revivals" (reforming of the packet after some time) are possible in bound systems, due to the quasi-periodicity of the quantum evolution, a consequence of the discreteness of the spectrum. Because of that "quasi" though, most of the times these revivals are only partial. The recent discovery of eigenstates behaving as (nondispersive) wavepackets themselves [4–6] is therefore of great interest and has spurred studies both theoretical [7] and experimental [8].

One semiclassical dynamical system accessible to experimental study where these particular "eigenstates" (actually very long lived resonances) have been found is the highly excited hydrogen atom exposed to a microwave electric field. An attractive characteristic of this system which makes it a convenient system for study is that if the atom is prepared in a static electric field collinear with the microwave field, and an extreme Stark state is excited, a one-dimensional approximation can be used, thus greatly simplifying the treatment.

The extended classical phase space (θ, I, t) of the one-dimensional hydrogen atom in a microwave electric field is approximately divided into a region of regular motion barely affected by the microwave field (field- modulated atom), a region dominated by resonance zones (nested vortex tubes surrounded by local chaos), and a globally chaotic region. In particular, when the ratio $\omega_0' \equiv n_0^3\omega/(1-3n_0^4F_S)$ of the microwave frequency ω to the initial Kepler orbit frequency $(1-3n_0^4F_S)/n_0^3$ (corrected for the static field F_S) is near unity, resonant classical motion dominates; we call this region of phase space the "principal primary resonance zone". Stroboscopic surfaces of section (Poincaré maps) reflect these zones in the full phase space as characteristic zones in the action-angle (θ, I) subspaces ("sectioned" phase spaces); in any such subspace a resonance zone appears as a chain of stable regions (islands) centered on stable periodic orbits and surrounded by a locally chaotic region containing unstable periodic orbits. The vortex tubes produce the resonance island zones and the local chaos produces the zones of irregular motion that have been called "separatrix" zones [9]: just like the separatrix in integrable problems, a chaotic layer -that grows with increasing microwave field strength- separates regions corresponding to different kinds of regular motion. The same type of structure is seen repeating itself within the primary resonance zones themselves, resulting in secondary resonance zones. The details of this picture change with the strength of the microwave field.

These classical zones in phase space are reflected in the character of the Floquet eigenstates (FE) [10]: regular FE are modulated atom FE or resonance island FE, supported by the nested vortex tubes of a resonance island chain. Noticeable among irregular FE are the separatrix FE, possibly "scarred" [11] by a high electron probability density in phase space along the unstable periodic orbits of the classical separatrices that support them [4, 12]. At intermediate values of microwave field strength, localization along the unstable periodic orbits is only partial and the FE extend over a bounded region of phase space classically occupied by chaotic trajectories [4, 10]. Ref. [4] shows that a field modulated FE is still similar to a free atom state: its configuration space wavefunction is almost stationary, there being no evident sign of significant oscillations. The FE supported by the center of the principal primary resonance zone is instead a **nondispersive packet** oscillating at the frequency of the microwave field, that is the frequency of the classical **stable** periodic orbit around which the state is localized [4]. The "packet" is most of the time quite

smooth, apart from some self interference when it is close to the nucleus, (the case of the surfaces of section in ref. [13], where the island is strongly deformed into a heart shape). This smoothness and almost Gaussian shape of the state is connected to the high field behaviour of the quasienergy levels of the principal primary quantum nonlinear resonance. In the high field limit they have a linear dependence on the "resonance quantum number" k (see ref. [14] and ref. therein), that is: they are equally spaced [15]. The system is therefore at least locally harmonic and the $k = 0$ quasienergy state supported by the center of the resonance is essentially the (Gaussian-shaped) ground state of a harmonic oscillator that, in the case of the principal primary resonance (the only case investigated up to now), is "forced" by the microwave field to oscillate at the frequency [4] of the microwave itself [16]. Ref. [6] attributes these forced oscillations to "a nonlinear coupling between the atom and the driving field that locks the electronic motion to the driving frequency" ; this phenomenon is known as **autophasing of the nonlinear oscillations** [17].

Finally a separatrix FE is a rather irregular **nondispersive packet** oscillating with the same period of the microwave, that is: following the classical **unstable** periodic orbit around which the state is localized [4]. The irregularity or "contamination" of the state is attributed by Ref. [4] to the flow of probability through the separatrix zone between the inside and the outside of the resonance. To view this quantum flow in phase space it is necessary to resort to some representation in phase space of the wavefunctions; Husimi functions have the advantage on the more commonly used Wigner functions of being positive defined. Husimi functions of states with support in the separatrix region between the separatrix state and the primary island sometimes display branches of probability extending to higher actions and a superposition of any of these Husimi functions over the separatrix Husimi function shows that these branches seep through the probability valleys that lay between the peaks of the separatrix Husimi function [4]. These valleys are therefore a suspected quantum equivalent of the separatrix "turnstiles" described in ref. [18] responsible for the classical flow of probability out of resonance zone.

The importance of these "scarred" separatrix wavefunctions is that with increasing microwave field strength their lifetime decreases much more slowly than that of the states whose support in phase space is within the resonance zone and for sufficiently strong fields becomes comparable to that of the ("Gaussian") state at the center of the resonance zone [4]. While the stability of the state at the center of the resonance zone brings about an agreement between quantum and classical behaviour ("classical" stabilization), the comparable stability of the "scarred" wavefunction in a region of chaotic classical behaviour causes a sharp divergence between quantum and classical behaviour ("quantum" stabilization).

The present paper deals with the possibility of selective population, starting from a highly excited hydrogen atom, of one such "separatrix" state at the peak of a partially ionizing short pulse of microwave electric field. I show that, taking care to avoid some critical cases, this is usually possible for the range of parameters of the laboratory experiments [14]. Previous studies dealing with this form of quantum stabilization [13, 19–21] concentrated on the sharp $\omega_0' \simeq 0.69$ maximum in the peak microwave field strength $F_0(10\%) = F(10\%)n_0^4$ (rescaled to the average Coulomb field on the Kepler orbit $1/n_0^4$) necessary for 10% ionization probability (see Fig. 1); I instead claim that it is the divergence between classical simulations (circles) and experimental results (triangles) over the whole region $\omega_0' \in (0.69, 0.85)$ that is due to the selective population of $\omega_0' = 1/1$ separatrix states [22]. The $\omega_0' \simeq 0.69$ peak itself only marks the "crossover" point where we pass from the $\omega_0' = 1/1$ resonance zone to the $\omega_0' = 2/3$ one. To the right of the $\omega_0' \simeq 0.69$ peak, the experimental $F_0(10\%)$ curve approximately corresponds to the initially populated quantum state evolving (at the peak of the pulse) into the $\omega_0' = 1/1$ separatrix state (a quantum adiabatic process). To the left of that same peak the initially populated quantum state is also the state at the center of the $\omega_0' = 2/3$ resonance zone. Not only adiabatic population of a single state at the center of a resonance zone might require a much longer switch-on time than adiabatic population of a state at the separatrix [20, 23], but (more important, as we shall see) for such a small resonance zone as the $\omega_0' = 2/3$ one, the state at the center of the resonance zone is less stable than the separatrix state.

The paper is organized as follows: in section II, I present the system and the numerical techniques I use to investigate it; the results of my investigation are presented and interpreted in section III. Section IV finally sums up my findings.

II. THE SYSTEM AND NUMERICAL METHODS

The system I investigate is a 1D model for a stretched highly excited hydrogen atom in collinear static and monochromatic microwave electric fields [14]. In atomic units the Hamiltonian reads

$$H = \frac{p^2}{2} - \frac{1}{z} + z[A(t)F^{max}sin(\omega t + \phi_0) - F_S], \qquad z \geq 0, \tag{1}$$

where $A(t)$ is the envelope of the microwave pulse. To simulate the experimental situation described in ref. [24], I have chosen

$$A(t) = \sin\left(\frac{\pi t}{T_p}\right)$$

where T_p is the length of the microwave pulse.

The Hamiltonian 1 has the following important scaling property: let c be an arbitrary constant, introducing the scaled variables $p' = cp$, $z' = z/c^2$, $t' = tc^3$, $H' = c^2H$ and the scaled parameters $F_0^{max} = c^4F^{max}$ (peak microwave field strength), $F_{S0} = c^4F_S$ (static field) and $\omega_0 = c^3\omega$ (microwave frequency), we again have

$$H' = \frac{p'^2}{2} - \frac{1}{z}' + z[\sin\left(\frac{\pi t}{T_p}\right)F_0^{max}sin(\omega_0 t' + \phi_0) - F_{S0}],$$

and Hamilton's equations are invariant in form. In this paper I present my findings in terms of classically scaled parameters, choosing the constant c to be the quantum number n_0 in which the system is initially prepared. To compensate for the Stark shift of the atomic frequencies I present my data in terms of the first order Stark corrected scaled frequency $\omega_0' \equiv n_0^3\omega_0/(1 - 3n_0^4F_S)$ [25].

A. CLASSICAL METHODS

I numerically solved Hamilton's equations of motion in the free-atom action angle variables (I, θ), valid when the electron's energy is negative:

$$z = 2I^2\sin^2(\xi/2),$$
$$p = (1/I)\cot(\xi/2),$$

where the eccentric anomaly angle $\xi(\theta)$ is defined by $\theta \equiv \xi - \sin\xi$. To avoid equations of motion containing terms that diverge as z approaches zero, a dummy time η was introduced, defined by the equation $dt \equiv (1-\cos\xi)d\eta$ [26]. The true time t increases monotonically with η. The integration was performed using a fixed step, fourth order Runge-Kutta routine [14]. The ensemble of initial conditions (θ_0, I_0) was chosen so that, to first order in Fs, the (classical) electron energy $E(0)$ be equal to the value of the energy of the experimentally prepared initial quantum energy eigenstate

$$-\frac{1}{2n_0^2} - \frac{3}{2}F_Sn_0^2 = E(0) = -\frac{1}{2I_0^2} - F_SI_0^2(1 - \cos\xi_0). \tag{2}$$

Given a value of $\theta_0(\xi_0)$, this equation determines a corresponding value of I_0.

Classical values for the "ionization" probability P_I at the end of the pulse were averaged over uniform distributions of the initial angle θ_0 and microwave field phase ϕ_0 as already described in ref. [14]. The "ionization" probability was the sum of two contributions. One was from trajectories that were terminated at some time during the pulse where the instantaneous value of the energy E exceeded the value $-2\sqrt{F_S}$ for rapid ionization in the static field alone. The other contribution was from trajectories whose final value of E corresponded to energies of quantum energy eigenstates, see equation (2) above, with quantum numbers outside the interval $[50, 90]$ of detection of the "survived" atoms [14]. Stroboscopic surfaces of section (Poincaré maps) in (θ, I) space were also computed for $A(t)F^{max}$ equal to various constants F. They revealed the (long-time) structures existing in phase space for the various values of F that were traversed during the microwave pulse. The comparison of instantaneous ensemble distributions in phase space with these surfaces of section, for various times t during the pulse has proven a useful tool for the understanding of the evolution of the ensemble itself [14, 24].

B. QUANTUM METHODS

The time evolution of the quantum system was evaluated by numerical integration of the Schrodinger equation with H given by eq.1 on a finite subset of the (bound) free atom basis $\psi_n(z)$ chosen large enough so that the probability reflected at the boundaries was small [26]. Given an initial state $\psi(z, 0) = \Sigma_nC_n(0)\psi_n(z)$, the equation for the evolution of the expansion coefficients $C_n(t)$ is

$$i\frac{dC_n(t)}{dt} = E_nC_n(t) + \mathcal{F}(t)\Sigma_mZ_{n,m}C_m(t),$$
$$\mathcal{F}(t) = (F(t)sin(\omega t + \phi_0) - Fs), \tag{3}$$

where $Z_{n,m}$ is the matrix element of the operator z between the states n and m. I approximated $\mathcal{F}(t)$ with the function $\mathcal{F}'(t) = \mathcal{F}(t)\Delta t\Sigma_k \delta(t - k\Delta t)$ that tends to $\mathcal{F}(t)$ for $\Delta t \to 0$ (in the sense that the integral of their difference over an arbitrary time interval goes to zero as Δt) [26]. I took into account the loss of probability induced by the static field by the substitution in equation (3) of E_n with $(E_n - i\Gamma_n/2)$, where the decay factors Γ_n are given by the $(3D)$ formula from ref. [27]. The above procedures involved a number of unphysical parameters that had to be carefully chosen as not to falsify the results of the integration. In particular, truncating the basis puts us in a "fuzzy box"; in absence of microwaves the potential is therefore a kind of "double well" where not only the width but also the depth of the second well varies with the number of levels considered. I discussed my choices in ref. [14].

1. Quasienergy curves

Like in the classical case, the dynamics at constant microwave amplitude can help understanding the pulsed dynamics. If $A(t)$ is a constant, Schrodinger's equation is a differential equation with time-periodic coefficients. Floquet's theory is therefore applicable [28] and tells us that the equation has solutions in the form

$$\psi_i(t) = \Phi_i(t)e^{-i\varepsilon_i t/\hbar}, \qquad \Phi_i(t+T) = \Phi_i(t)$$

where T is the period of the microwave, the constants ε_i take the name of quasienergies and the functions $\psi_i(t)$ are called quasienergy (or Floquet) states. For periodic systems quasienergies take the place of energies in the description of the dynamical properties of the system. As quasienergies shifted by $2\pi\hbar/T$ with respect to each other correspond to the same physical state $\psi_i(t)$, it is sufficient to restrict ourselves to the energy interval $[0, 2\pi\hbar/T)$ (first Brillouin zone) to have all the levels. To calculate the quasienergies I resorted to the time evolution operators $G(\phi)$ over one period T of the microwave (Floquet operators), parametrized by the phase $\phi = (\omega t_0 + \phi_0)$ of the field at the beginning of the period. While the eigenfunctions $\Phi_i(\phi)$ of each member of the family are different and represent the different spatial structures of the states at different times during the microwave period, the family shares the same eigenvalues G_i, connected to the quasienergies by the relationship $G_i = e^{-i\varepsilon_i T/\hbar}$. To obtain the quasienergies I therefore numerically calculated a one period evolution operator and diagonalized it; the above equation then gave us the quasienergies on the circle $[0, 2\pi\hbar/T)$.

Plots of the quasienergies as functions of the microwave field strength F, called **quasienergy curves** (see Fig. 2), help us connect the characteristics of the system at different values of the microwave field strength. The quasienergies change with F and undergo a sequence of avoided crossings of widely different widths. Since in the $1D$ hydrogen atom all the quasienergies fall into the same symmetry class [29], the Von Neumann-Wigner theorem [30] tells us that they all repel each other; this implies the absence of real level crossings. As in our simulations of the pulsed system, we calculate the Floquet operator on a truncated basis and some caution has to be exerted to avoid spurious results. A study of the quasienergy curves themselves can help us in deciding what parts of what curves to believe [14, 31, 32].

2. Husimi function

When studying semiclassical systems, one wishes to understand to what extent phase space classical stuctures can guide the quantum evolution. To this end it is useful to have some representation of wavefunctions in phase space. One of the most widely used such representation is the Husimi function [33]. Given a quantum function $\psi(t)$, its Husimi function at a point $\{\langle p\rangle, \langle q\rangle\}$ in phase space is the projection (in atomic units) $\rho_H(\langle p\rangle, \langle q\rangle, t) = |\left\langle \phi_{\langle p\rangle\langle q\rangle} | \psi(t)\right\rangle|^2$ of $\psi(t)$ on a minimum uncertainty packet centered on that point in phase space and called the "coarse graining function". In action-angle space, due to the periodicity in the angle variable, the standard (position-momentum space) choice of coarse graining function [32] is not possible. Following ref. [11] I therefore take

$$\phi_{\langle I\rangle\langle\theta\rangle} = \Sigma_{n=0}^{\infty}\left[\frac{\alpha^{(\alpha n+1)}}{2\pi\Gamma(\alpha n+1)}\langle I\rangle^{\alpha n} e^{-\alpha\langle I\rangle}\right]^{1/2} e^{i2\pi\langle\theta\rangle n}\psi_n.$$

Tests with different values of $\alpha < n_0$ have given (both for ref. [13] and for me) Husimi functions having essentially the same shape. The comparison of the Husimi function of the wavefunction at various times of the microwave pulse with the classical ensemble at the same times and with the classical surfaces of section at the same values of ω, F and ϕ_0 can often be quite instructive.

III. RESULTS

A. QUANTUM ADIABATIC BEHAVIOUR AT THE SEPARATRIX BAND

The behaviour of a grouping of strongly interacting levels (repelling each other) at, or close to zero microwave field, is particularly evident in Fig. 2. I have marked them as darker lines. The (zero microwave field) energy of each of these levels is close to a quantum resonance $\Delta E \equiv E_{n+r} - E_n = s\omega\hbar$ with any of the other levels of the same grouping; the ratio s/r being equal to 1 for any two levels of the grouping. This grouping represents on the (E, F) plane what ref. [34] calls a nonlinear quantum resonance : a finite (because of level anharmonicity) number of quantum states whose interaction is due to the existence of a (primary) classical resonance zone, in this case the $\omega_0' = 1/1$ resonance zone. The levels initially curve downwards, reach a minimum and then start growing at a fast rate; the inflection point of a curve indicates where the character of the state changes from field modulated free atom to resonance state [14]; the transition is drastic (see appendix B) and is characterized by a change in semiclassical WKB quantization [14]. At lower microwave field strengths the quantum number is the free atom one, n; while for higher fields the quantum number is the "resonance" one, $k = 0, 1, 2...$ The $k = 0$ state at the center of the quantum linear resonance being the one with the fastest growing quasienergy. Therefore the inflection point is where we can find a separatrix state. If, for the pulsed system we are considering, we want to selectively populate such a state at the peak of the pulse, we must choose an initial state such that the quasienergy curve originating from it has its inflection point close to the peak of the pulse itself.

As an example to be viewed through Figure 2, let us consider a Hydrogen atom prepared in an extreme Stark state with principal quantum number $n_0 = 65$ in a static field $F_S = 8 \;\; V/cm$, and subject it to a microwave pulse with $\omega = 18.00 hspace.1 in GHz$, and $F^{max} = 4.63 \;\; V/cm$, lasting $T = 140$ microwave periods; rescaled, the parameters of the microwave and static fields are $\omega_0' = 0.8196$, $F_0^{max} = 0.01607$ and $F_{S0} = 0.02777$. The principal primary resonance is centered at $n_r = 69$ and according to the equation at the top of page 2185 of ref. [20], at the peak of the pulse the resonance contains

$$N = \frac{8 n_r}{\pi} \left(\frac{0.325 F_r^{max}}{3(1 + F_{rs})} \right)^{1/2} = 8$$

quantum states (see appendix A for a discussion of the small difference between the present formula and the one in ref. [20]). A look at the zero microwave field "quasienergies" moreover shows that these 8 states are the states $n = 65$ to $n = 72$. A classical ensemble simulating at $t = 0$ the quantum Stark state $n_0 = 65$ will therefore enter the resonance zone close to the peak of the pulse, as can be seen in Fig. 3 which shows snapshots of the classical ensemble near the peak and at the end of the pulse: the ensemble enters the primary resonance zone after about 55 periods of the microwave, when the field strength is about 94% of peak. The full line in Fig. 4 shows the final distribution in action that is, as expected [35], double peaked in action with one peak centered on $n_0 = 65$ and the other one centered on its "symmetric" action ($n_s \simeq 73$) with respect to the center of the island ($n_r = 69$). It is also evident, both from Fig. 4 and from the last snapshot of Fig. 3, that the two peaks are rather wide and of quite different shapes. Even if there is no noticeable spread in action at the crossing itself, the width of the peaks comes as no surprise if we consider the wide chaotic separatrix region over which the ensemble is spread at the peak of the pulse (see the snapshot at $t = 70$ microwave periods in Fig. 3). The asymmetry in shape of the two peaks takes the form of an approximately exponential fall of the population distribution for $n > n_0 = 65$, superimposed over the double peak structure (see Fig. 4). This shape suggests a coupling of the chaotic band to the global chaos above as the cause of the asymmetry [36]. Since the presence of the $\omega_0' = 2$ resonance zone below the static field ionization threshold does not allow direct static field induced escape from the local chaotic band, the calculated ionization probability $P_I = 21.3\%$ confirms the above view.

A quantum simulation at the same parameters gives a much lower second peak at $n_s = 73$ (see the dashed curve in Fig. 4 and notice the vertical logarithmic scale) and negligible ionization probability, suggesting an (almost) adiabatic quantum evolution. Even more suggestive is a comparison of the evolution of the classical and quantum population on the Stark levels during the pulse: the two distributions are quite different even at early times: quantum transfer of probability to levels around $n_s = 73$ grows steadily during the rise of the pulse while in the classical system we have a sudden spread of the probability after about 60 microwave periods. At the peak of the pulse, classical and quantum distributions on the Stark states again appear similar; but the differences increase and become dramatic when, during the fall of the pulse, we get to the second separatrix crossing and most of the quantum population returns to the initial state. While it is only from the second crossing on that we get a fundamental divergence between classical and quantum behaviour, we do have significant classical-quantum differences at both crossings, reflecting the fact that it is near the separatrix that classical and quantum systems are most different. At the separatrix a classical frequency goes to zero [37], thus forbidding any adiabatic evolution through the separatrix, but no quantum frequency (usually)

goes to zero, so that adiabatic evolution is possible [32, 38]. Indeed at the peak of the pulse only two quasienergy states are significantly populated: most of the probability (94.6%) is still on the (separatrix) state "adiabatically" connected to the $n_0 = 65$ initial state; almost all of the rest (5.1%) is on the $n = 77$ state (dashed line in Fig. 2) that right at the peak of the pulse has a (narrow) avoided crossing with the $n_0 = 65$ state. As expected for an almost pure "separatrix" state the Husimi function of the wavefunction at the peak of the pulse is localized over the separatrix region of the classical $\omega_0' = 1/1$ resonance zone: see Fig. 5 where the Husimi function is superimposed over the classical surface of section. I tested the stability of the state thus excited by inserting a long (600 microwave periods) flat central section to the microwave pulse. Even if the state is not right at the separatrix (the Husimi function of a true "separatrix" state should have a peak centered on the unstable fixed point, while in Fig. 5 that peak has already begun to split in two, each of these peaks closer to the center of the resonance zone than the unstable fixed point), it displays remarkable stability: a numerical fit of a two-terms exponential decay model to the ionization probability during the flat central region of the pulse gives a half lifetime of about 2700 microwave periods for the main component (about 95%) against about 240 microwave periods for the remaining 5%.

To check whether evolution on a single (long lived) quasienergy state is the general behaviour for quantum states near $n_0 = 65$ at the same classical conditions, I have performed quantum calculations at the same scaled parameters but at different values of n_0 in the range $n_0 \in [57, 73]$. In all cases we have significant spread of the population at the peak of the pulse and very sharp peaks at the end. Significant peaks away from n_0 (the biggest one always on n_s, its "symmetric" state with respect to the center n_r of the principal primary resonance [39]) are visible only for $n_0 = 59$, 60, 67, 68 and 73. These are also the only cases where significant ionization takes place as can be seen in Fig. 6.a. These sharp ionization peaks as a function of n_0 and the equally sharp peaks in the final population distributions both tell us that for these values of n_0 and of the peak microwave field F^{max} (and we should also include the pulse time T) quantum effects are essential: we are still away from the hard semiclassical limit where multilevel interactions dominate [40]. Indeed Fig. 6.a can be explained by two level quantum resonances: Fig. 6.b plots (versus n_0 and in units of $\hbar\omega$) the difference between the zero microwave field quasienergies of n_0 and n_s: the ionization peaks correspond to the minima of this difference. As a further test of the two level character of the interaction responsible for the peaks, Fig. 6.c shows the very good fitting of the Demkov model eq. (C1) to the numerically calculated population that has left n_0 at the end of the pulse. For simplicity I have assumed the parameters V_0 and B^2 to be n_0-independent so that eq. (C1) reads $P^{(2)}_{a->b} = K_1/cosh^2(\Delta/K_2)$ where Δ is the quantity plotted in Fig. 6.b and the two fitted parameters are $K_1 = 0.8337 \pm 0.0001$ and $K_2 = 0.01756 \pm 0.000005$. As a last test of the above interpretation I have calculated the projection of the wavefunction at the peak of the pulse on the instantaneous quasienergy states for the case $n_0 = 67$ (that from Fig. 6.b is one of the two minima of the difference between the zero microwave field quasienergies of n_0 and n_s). The crosses on the quasienergy curves in Fig. 7 indicate the most populated eigenstates: 39.1% of the population is on the $n = n_0 = 67$ state and $23.4 + 16.6\%$ on the state $n = n_s = 75$ undergoing at that field value a narrow avoided crossing with a "second well" state (dashed line). Using the above eigenstates as initial conditions for integration of the Hamiltonian (1) with $A(t)$ a constant I obtained their half-lifetimes: the longest lived state is the $n = 67$ one (about 300 microwave periods), the other two states display an initial fast decay of their "second well" part (about 30% of the $n = 75$ state and 70% of the other decays with a lifetime of about 10 microwave periods) followed by a decay corresponding to a lifetime of about 160 microwave periods. Both the peak microwave field quasienergy states $n = 67$ and $n = 75$ therefore have half lifetimes about one order of magnitude smaller than the $n = 65$ almost "separatrix" state. This reduced lifetime is likely to be reflected in Husimi functions of the eigenstates considered. Moreover, as the main interaction is between two states belonging to the principal primary quantum nonlinear resonance, it is reasonable to assume that local characteristics of the Husimi functions in the region of phase space of the principal primary resonance zone will be relevant. Since the spacing of semiclassical quasienergy curves quantized according to the resonance quantum number k is approximately uniform, whenever two zero microwave field quasienergies are degenerate (or almost degenerate) the shift of the two k-quantized quasienergy curves from the continuation of n-quantized ones has maximum (see for example in fig 10 of ref. [14] the lengths of the segments connecting the inflection points of the quasienergy curves calculated in the two quantizations). This strong repulsion of the two quasienergies corresponds to a substantial mixing of the two states; using the terminology of ref. [41] they are "dirty". The matter is now to recognize a "dirty" state from a "clean" one. To this end we note that "quantum resonance" means that a quantum frequency is zero; therefore, just like it happens at the separatrix in the classical system, adiabatic evolution becomes impossible (or, in the case of almost degeneracy, requires very long times). This common characteristic of the two systems is reflected in the somehow similar behaviour of the two systems we see for $n_0 = 59$, 60, 67, 68 and 73. Since scarring of the separatrix state is the one quantum states' characteristic associated (at least at constant microwave field amplitude) with strong deviations from the classical behaviour, it appears likely that the scarring of these "dirty" states (when, at some time during the pulse they become separatrix states) will be less pronounced than usual. Figure 8.a shows for $n_0 = 67$ the Husimi function of the wavefunction at the peak of the pulse: it shows a very different picture than the peak Husimi function for $n_0 = 65$ (Fig. 5). The maximum is still close to the classical unstable fixed point, but the low, smooth ridge

surrounding the classical primary resonance zone is now marred by the presence of two very noticeable peaks. The Husimi functions of the three eigenstates making up much of the instantaneous wavefunction (Fig. 8.b) show that these two peaks are part of the $n = n_0 = 67$ eigenstate. All three eigenstates have their maximum near the unstable fixed point but as expected no eigenstate is exclusively localized around the unstable fixed point. The closest we get to this condition is with the Husimi function of the $n = n_s = 75$ eigenstate whose quasienergy, as we can see from Fig. 7, falls close to the inflection point of its quasienergy curve. The quasienergy of the $n = n_0 = 67$ eigenstate instead appears to fall to the right of the inflection point of its curve and accordingly its Husimi function appears squeezed toward the center of the principal primary resonance zone. Also, in this case, the ridge surrounding the classical principal primary resonance zone is absent from the Husimi functions of all three eigenstates. In its stead the $n = n_s = 75$ eigenstate has two low peaks approximately in the same position of the much higher peaks of the Husimi function of the "second well" eigenfunction. These peaks -in their turn- alternate with the peaks of the $n = n_0 = 67$ eigenstate. These correspondences and alternations (together with the knowledge that away from avoided crossings the support of the "second well" state is far from the principal primary resonance zone) lead us to believe that in absence of the avoided crossing with the "second well" state, the "separatrix" state would have (in the region of the principal primary resonance zone) a Husimi function equal to the sum of the $n = n_s = 75$ one and the "second well" one. That is: a wavefunction with noticeable peaks away from the unstable fixed point. Our next step will be to try and locate, in the plane (ω_0', F_0^{max}) of rescaled frequency ω_0' and peak microwave field strength F_0^{max}), the range of parameters where the adiabatic behaviour of the quantum states at the separatrix we have just described results in the quantum ionization probability being lower than the classical one. We call this enhanced lifetime of the atom "quantum stabilization".

B. SIGNS OF QUANTUM STABILIZATION IN THE EXPERIMENTAL IONIZATION DATA

Figure 1 compares the scaled experimental peak microwave field strength for 10% ionization $F_0(10\%)$ (triangles) [14] with the same quantity from classical numerical simulations (circles): starting from $\omega_0' \simeq 0.85$ and down to $\omega_0' \simeq 0.60$ both curves show an increase in $F_0(10\%)$ but the experimental $F_0(10\%)$ grows faster and the sharp peak at $\omega_0' \simeq 0.69$ is clearly non classical. The classical part of this increase can be easily explained: to be able to ionize, the ensemble must first enter the chaotic "separatrix band" surrounding the principal primary resonance island. This can be easily seen from a comparison of the classical $F_0(10\%)$ with the fields at which classical ensembles with initial conditions at various values of ω_0' enter the primary resonance zone (dots in Fig. 1): the two are almost identical. Both of the classical numerical curves in Fig. 1 are lower than the evaluation of the separatrix action location in asymmetric pendulum approximation eq. A2 (heavy curves in Fig. 1) that instead matches very well the $F_0(10\%)$ experimental data. The peak at $\omega_0' \simeq 0.69$ moreover appears to be right at the intersection of the $\omega_0' = 1/1$ separatrix location curve with the separatrix location curve of the $\omega_0' = 2/3$ resonance zone. Eq. A2 is an approximation that, as I explain in appendix A, only keeps the locally (in phase space) resonant term in the Fourier expansion in the angle variable θ of the interaction term between the electron and microwave field. The agreement of the experimental data with it might therefore be fortuitous; on the other hand I do suspect it to be significant. Let us start by looking at some surfaces of section, choosing the parameters along the experimental $F_0(10\%)$ curve. Fig. 9 shows the surface of section at a point to the far right of Fig. 1 where all the curves we have seen approximately agree. The chaotic band is already rather well developed and, as expected by the nonzero ionization probability, already extends to high actions. On the other hand the manifolds of the unstable fixed point still show oscillations only very close to the fixed point itself (visible in the upper separatrix band on the right hand side of the figure); it is therefore rather easy to draw an approximate "separatrix curve" that cuts through these oscillations. It is immediately clear that while at the upper separatrix the chaotic band extends on both sides of the "separatrix curve", at the lower separatrix it is mostly confined to the inner side. Therefore, if we approach the resonance zone from below, entering the chaotic band will be equivalent to crossing the "separatrix curve". Fig. 10.a shows instead a surface of section right at the $\omega_0' \simeq 0.69$ peak: the upper manifolds now oscillate wildly and drawing an approximate "separatrix curve" becomes less intuitive [18], but it is still possible to draw an intuitive approximate lower separatrix curve (dashed line in Fig. 10.b). The inner side of the chaotic band is still bigger, but now the outer side is substantially thick (and merged with the chaotic band enveloping the $\omega_0' = 2/3$ resonance zone). This time, approaching the resonance zone from below, we first enter the chaotic band and then cross the "separatrix curve". This explains in all likelihood the disagreement of eq. A2 with the field for entrance into the primary resonance zone, but what about the agreement of eq. A2 with the experimental results? We know that the unstable fixed point and its manifolds may support a scarred state and that this state can be quite stable [4]. The curve from eq. A2 (obtained approximating these manifolds with a "separatrix curve") gives us the position in the (ω_0', F_0) plane of this "separatrix" state. Below that curve we expect to find modulated free atom states; above, fast decaying states with Husimi functions supported by the inner chaotic band [42]. The picture we have for our pulsed system is therefore the following: for classical ionization to happen it

is enough to enter the chaotic band (assuming that at some point during the pulse that same chaotic band merges with the local chaos above), but for significant quantum ionization the quantum state must evolve past the scarred separatrix state. The $\omega_0' \simeq 0.69$ peak in the experimental $F_0(10\%)$ would then only represent the "point" in ω_0' where we pass from selectively populating at the peak of the pulse the $\omega_0' = 1/1$ separatrix state to populating some (less stable) state of the $\omega_0' = 2/3$ resonance zone; we shall see that this state is the state at the center of the $\omega_0' = 2/3$ resonance zone. The quantum $F_0(10\%)$ for a number of cases is shown in Fig. 11, compared with the corresponding classical and experimental $F_0(10\%)$. Even if somehow lower in height and shifted to lower frequencies ($\omega_0' \simeq 0.682$ instead than $\omega_0' \simeq 0.687$) the quantum peak seems in reasonable agreement with the experimental one. To confirm my supposition on the origin of the $\omega_0' \simeq 0.69$ peak, I have calculated the projections of the wavefunction on the instantaneous Floquet eigenstates at each period of the microwave during the first half of the pulse for two cases along the quantum $F_0(10\%)$ curve at the two sides of the peak: $\omega_0' = 0.675$ and 0.685; $F_0 = 0.04$ in both cases, but the field rescaled to the action at the center of the resonance zone (see appendix D) is in the latter case 2% lower. They are shown in Figs. 12.a and 13.a. Figs. 12.b and 13.b show instead the quasienergy curves: I have marked as darker lines the quasienergy curves of the $s/r = 1/1$ nonlinear quantum resonance (full lines) and (dashed lines) the two groupings of levels of the $s/r = 3/2$ one; the central state (in the free atom quantum number n) of each grouping is the top one in the graph. For $\omega_0' = 0.675$, immediately to the left of the quantum $F_0(10\%)$ peak in Fig. 1, we see in Fig. 12.a that only at the peak of the pulse the initially populated $n_0 = 65$ state ("central" state of the top $s/r = 3/2$ grouping and $k = 16$ state of the principal primary resonance) has a crossing with its nearest $s/r = 3/2$ state ($n = 63$). Most of the population is therefore still on a $s/r = 3/2$ "island" state as can be clearly seen from the Husimi function at the peak of the pulse, shown in the top part Fig. 14, superimposed over the classical surface of section at that same time: the maxima of the Husimi function are over the two classical $s/r = 3/2$ islands. At the bottom the same figure are shown the Husimi functions of the three eigenstates on which the instantaneous wavefunction has the highest projections: most of the population (62.3% + 15.7%) is on two states having their maxima over the two islands of the $\omega_0' = 2/3$ resonance zone (in the order: $n = 65$ and the self ionizing state [43] having at that point a narrow avoided crossing with it) and only 12.7% is on the $n = 63$ state, localized on the two unstable fixed points of the same resonance zone. To the right of the peak we instead see in Fig. 13 that the $n_0 = 65$ and $n = 63$ states cross at $F_0 \simeq 0.026$; at the peak of the pulse most of the population is now on a state having the same character with respect to the $s/r = 1/1$ resonance as in the case above but that now is the second state of the top $s/r = 3/2$ grouping. The maxima of the Husimi function at the peak of the pulse are therefore no more over the islands of the $\omega_0' = 2/3$ resonance zone but have moved over to the two unstable fixed points as can be seen in Fig. 15.a. The Husimi functions of the two eigenstates on which the instantaneous wavefunction has the highest projections (Figure 15.b) are again localized, one (61.6% of the population) around the two unstable fixed points and the other (19.3% of the population) over the two islands of the $\omega_0' = 2/3$ resonance zone. In conclusion, at both sides of the $F_0(10\%)$ peak we have more than 60% population on a single eigenstate but their character is quite different as can also be seen from their lifetimes. At $\omega_0' = 0.685$ the most populated state is a $\omega_0' = 2/3$ "separatrix" state with a lifetime of about 210 microwave periods while at $\omega_0' = 0.875$ the most populated state is a $\omega_0' = 2/3$ "island" state with a lifetime of only about 40 microwave periods. It is interesting to note that while the lifetime of the "separatrix" state only decreases from about 210 to about 180 microwave periods when going from $\omega_0' = 0.685$ to $\omega_0' = 0.675$, the lifetime of the "island" state decreases from about 580 microwave periods to only 40. If we attribute these decreased lifetimes to the slight increase the microwave field strength rescaled to the action at the center of the resonance we noted above, this behaviour would be in agreement with the findings of ref. [4] for the $\omega_0' = 1/1$ resonance zone: there it was noted that with increasing microwave field strength the lifetime of the "separatrix" states decreases much more slowly than the lifetime of the "island" states.

IV. CONCLUSIONS

I have shown that, starting from a highly excited ($n_0 \simeq 65$) hydrogen atom and taking care to avoid some critical cases, it is indeed possible to selectively populate one long-lived "separatrix" state at the peak of a partially ionizing short pulse of microwave electric field such as the ones used in the laboratory experiments [14] . This nonclassical quantum adiabatic behaviour is due to the still low density of the resonance quasienergy levels that allows the relevant quantum transition frequencies to be much faster than the field strength change rate. On the other hand, the spacing of these principal quantum nonlinear resonance quasienergy levels for vanishing microwave field strength is not uniform and care must be taken to avoid starting from a state close to a (zero microwave field) two level quantum resonance with one of its two nonlinear resonance neighbours. If the relevant quantum frequency becomes comparable to the rate of change of the field strength then adiabatic behaviour is no more possible: the "local" increase in the density of resonance states has made the system more semiclassical. I have also shown that the sharp $\omega_0' \simeq 0.69$ maximum in $F_0(10\%)$ (on which all previous studies dealing with this form of quantum stabilization [13, 19–21] concentrated)

only marks the "crossover" point from the $\omega_0' = 1/1$ resonance zone to the $\omega_0' = 2/3$ one. It is instead the whole region $\omega_0' \in (0.69, 0.85)$ that shows clear signs of the quantum stabilization induced by the selective population of the separatrix state: with decreasing frequency the divergence between the quantum (and experimental) and the classical $F_0(10\%)$ increases. I have shown that this divergence is due to the increase in the width of the classical chaotic "separatrix" band: for classical ionization to happen it is enough to enter the chaotic band, but for significant quantum ionization the quantum state must evolve past the scarred separatrix state. The stability of the separatrix state itself appears instead from my calculated lifetimes to decrease with decreasing frequency.

V. AKNOWLEDGEMENTS

The author wishes to thank C. Rovelli, G. Mantica and S. Locklin for useful comments and suggestions and the latter also for the use of his computer for the quantum numerical simulations presented in this paper. Special thanks to J.E. Bayfield as advisor of my Ph. D. thesis, amply quoted in the present paper.

APPENDIX A: CLASSICAL PENDULUM APPROXIMATION FOR THE SEPARATRIX LOCATION CURVE [22]

When $A(t)$ is a constant, one procedure often used to study the Hamiltonian (1) is to locally approximate it with an integrable one around any resonant action Ir defined by $\omega I_r^3/(1 - 3F_S I_r^4) = s$ where s is an integer [44]. In brief: we first substitute the atom-static field interaction term with its average over one free atom period [45]. Then, the free atom Hamiltonian is expanded in powers of $x = (I - I_r)$ up to the second order term and the atom-field interaction term is Fourier expanded in the angle variable θ. All terms of the latter expansion but the s-th one average to zero over one period of the microwave field; they can therefore be neglected in first approximation. The fast motion with frequency ω can be extracted by a canonical transformation canceling the time dependence of the interaction term; this will also cancel the linear term in the expansion of the free atom Hamiltonian thus leaving us with the Hamiltonian of a pendulum describing the slow motion inside the resonance island

$$H^{(2)} = -\frac{3(1 + F_S I_r^4)}{2I_r^4} x^2 - F I_r^2 \frac{J_s'(s)}{s} \cos s\theta \tag{A1}$$

where $J's(s)$ is the derivative of the Bessel function J. The above Hamiltonian highlights the component of the interaction responsible for the most noticeable structures in phase space, namely the primary island chains corresponding to free atom rotation numbers $1/s$. As costumary, we shall use the approximation $J_s'(s)/s \simeq \mu/s^{5/3}$ [46], where $\mu = 0.325$ if $s = 1$ and tends to $\mu = 0.411$ for $s \to \infty$. From the Hamiltonian A1 it is then easy to obtain the equation in phase space of the separatrix between rotational and librational motion. Since the action associated with an invariant curve $I(\theta)$ is the integral in $\theta \in [0, 2\pi)$ of $I(\theta)$ divided by 2π, calling $\mathcal{A}^{\pm}$ the two integrals for the upper and lower separatrix, the two actions

$$I^{\pm} = I_r \pm \frac{\mathcal{A}^{\pm}}{2\pi}$$

are the actions just above the upper separatrix (I^+) or just below the lower separatrix (I^-).

In the limit of very slow rise of the pulse the action is an invariant; in that limit $I^{\pm}$ therefore represent, for an atom in a pulsed microwave field with peak microwave field strength F, the free atom actions of points that are at the separatrix at the peak of the pulse. We call them the "separatrix actions" of the resonance zone. This derivation is discussed in ref. [20]; but there the interaction term of the pendulum Hamiltonian contains a higher order correction to the atom-microwave interaction term that I think inconsistent with a first order approximation in both F and F_S. A modified pendulum approximation for the slow component of the regular motion inside the resonance island can be used to take into account the asymmetry in action of the resonance zone; in this new approximation the expansion of the $-1/2I^2$ term in the Hamiltonian around the resonant action I_r is carried one term further [47]. Including both the first order static field correction and the asymmetry term, my calculation yields the following formula in the case of the $\omega_0' = 1$ resonance zone:

$$I^{\pm} I_r = 1 \pm \frac{4}{\pi} (B F_r)^{1/2} + \frac{4}{3} \frac{B F_r}{(1 + F_S^r)},$$

where $B = 0.325/[3(1+F_S^r)]$. Here F_S^r is the static field scaled by I_r^4. This equation can be used to obtain a "separatrix location function" in the (ω_0', F_0) parameter space which, expressed in terms of the parameter $u_\pm = I_r/I^\pm$, is:

$$\omega_0'^{\pm} = s\frac{1-3F_{S0}u_\pm^4}{(1-3F_{S0})u_\pm^3}$$
$$F_0^\pm = \left(\frac{1-\left[1-\mathcal{W}\left(1-\frac{1}{u_\pm}\right)\right]^{1/2}}{\mathcal{W}V}\right)^2 \tag{A2}$$

where

$$\mathcal{V} = \frac{2}{\pi}\left[\frac{\mu u_\pm^4}{3s^{5/3}(1+F_{S0}u_\pm^4)}\right]^{1/2}$$

and

$$\mathcal{W} = \frac{\pi^2}{3(1+F_{S0}u_\pm^4)}.$$

APPENDIX B: CLASSICAL AND QUANTUM CHANGE OF BEHAVIOUR AT THE SEPARATRIX [22]

To stress the importance of the inflection point of the quasienergy curves as the transition point between two very different types of quasienergy states, ref. [48] calculated the time-independent expectation value of the unperturbed Hamiltonian H_0 on the quasienergy states themselves:

$$H_0^{k,k} = < \phi_k(z,t)|H_0|\phi_k(z,t) > = \Sigma_n a_{kn}^2 E_n \tag{B1}$$

there is a fast change of behaviour at a value of k that in each case is in good agreement with $k_{max} = 8(0.325F/3)^{1/2}/\pi\omega - 1/2$. To the right of that point $H_0^{k,k} \simeq E_{n(k)}$ (the unperturbed energy of the corresponding $n(k)$), meaning that the only coefficients in eq. (B1) significantly different from zero are $a_{kn(k)}$ and the a_{kn} with n close to $n(k)$, that is: only states on the same side of the resonant state R give a significant contribution in (B1). To the right, $H_0^{k,k}$ decreases with increasing k but remains close to the energy E_R of the resonant state: the significant coefficients a_{kn} in the sum (B1) correspond now to n's both below and above R. This behaviour is present also in the classical description and the two limiting behaviours can be easily understood as follows: outside of the resonance zone the motion is still very similar to the unperturbed one, so that the average atomic energy $< H_0 >$ for a given orbit remains close to the free atom one. Inside the resonance zone the motion is the sum of a fast component, that is the motion of the stable resonant orbit at the center of the resonance zone, and of a slow one around that same orbit resulting in the weak dependence of the energy $H_0^{k,k}$ on k. The slow motion determines in the quantum picture the spatial structure of the states, the fast one appears instead as oscillations in time, locked to the driving field frequency and in phase with the oscillations of the stable periodic orbit at the center of the resonance zone. It is possible to formalize this intuitive classical picture as follows: we again make use of the pendulum Hamiltonian (A1) and to keep the notation light we pass to rescaled variables and limit ourselves to the main resonance $s = 1$:

$$H = -\beta\frac{x^2}{2} + \alpha\cos(\theta)$$
$$\beta = 3(1+F_S I_r^4) \qquad \alpha = 0.325F_0$$

With this notation the average on a given orbit of the free atom energy is:

$$\langle H_0\rangle = -\left\langle\frac{1}{2I^2}\right\rangle \simeq -\frac{1}{2I^2} + \frac{\langle x\rangle}{I_r^3} + \left\langle H_0^{(1)}\right\rangle$$

where $H_0^{(1)} = -\beta x^2/2$ and the averages are calculated over the pendulum invariant curves. Both $\langle x\rangle$ and $H_0^{(1)}$ change markedly when passing from inside to outside the separatrix. Inside the separatrix we have

$$\langle x\rangle = 0 \tag{B2}$$

and outside (the + sign will of course be for orbits above the separatrix and vice versa):

$$\langle x\rangle = \pm\pi(\alpha/\beta)^{1/2}/R\mathbf{K}(R) \tag{B3}$$

where $R = (2/(1-H/\alpha))^{1/2} = 1/|sin(\Theta/2)|$, Θ being the (half) amplitude in θ of the oscillations, and $\mathbf{K}$ is a complete elliptic integral [49]. Expression B3 is zero for $R = 1$(at the separatrix) and for $R \to 0$ becomes

$$\langle x\rangle = \pm(2|H_0|/\beta)^{1/2} \equiv \pm J \tag{B4}$$

The transition happens very fast and close to the separatrix: already at $R = 0.95$ the ratio $|\langle x\rangle/J|$ is about 0.87. Outside the separatrix, $\left\langle H_0^{(1)}\right\rangle = -J\pi(\alpha\beta)^{1/2}/2R\mathbf{K}(R)$ similarly shows a sudden transition: it is again zero at the separatrix and for $R \to 0$ it becomes

$$\left\langle H_0^{(1)}\right\rangle \simeq -|H_0| = -\beta J^2/2; \tag{B5}$$

but already at $R = 0.95$ the ratio $|\left\langle H_0^{(1)}\right\rangle/(\beta J^2/2)|$ is about 0.87. Inside the separatrix $\left\langle H_0^{(1)}\right\rangle = -J\pi(\alpha\beta)^{1/2}/4\mathbf{K}(1/R)$ that for $1/R \to 0$ goes as

$$\left\langle H_0^{(1)}\right\rangle \simeq -J(\alpha\beta)^{1/2}/2, \tag{B6}$$

has a minimum for $1/R \simeq 0.94$, where the ratio $\left\langle H_0^{(1)}\right\rangle/(\beta(J/2)^2/2)$ is about -1.205 and becomes zero at the separatrix. Summarizing, $\langle x\rangle$ grows suddenly when crossing from inside to outside the separatrix, $\left\langle H_0^{(1)}\right\rangle$ has a sharp dip at the separatrix itself. Far from the resonance zone we shall therefore have from eqs. (B5) and (B6)

$$\langle H_0\rangle \simeq -\frac{1}{2I_r^2} \pm \frac{J}{I_r^3} - |\Delta_k(0)| = -\frac{1}{2I_r^2} \pm J\omega - |\Delta_k(0)|;$$

it is now sufficient to remember that $|\Delta_k(0)| = |E_n - E_R - (n-R)\omega|$ and notice that, outside of the resonance zone, $J = |n-R|$, to obtain, in agreement with the quantum result in ref. [48], $\langle H_0\rangle \simeq E_n$. Close to the center of the resonance zone we shall instead have, from eqs. (B2) and (B4):

$$\langle H_0\rangle \simeq -\frac{1}{2I_r^2} - \frac{k+1/2}{2I_r}(0.975F)^{1/2}$$

that for each of the three figures in ref. [48] gives us slopes in good agreement with the numerical quantum results. The main difference between inside and outside the resonance zone, and the cause of the sudden jump in the behaviour of $H_0^{k,k}$, is clearly the term in $\langle x\rangle$ that is exactly zero inside the resonance zone (at least in pendulum approximation) and has a finite value immediately out of it. Its being zero inside the resonance zone is an expression of that locking of the resonance states' oscillation frequency to the microwave one I mentioned above [50].

APPENDIX C: THE DEMKOV MODEL

The Demkov model [51] deals with the interaction of two levels and assumes the two diabatic levels to be constant and the interaction between them to change exponentially with the perturbation parameter λ. Assuming the time to vary between $-\infty$ and $+\infty$ the Hamiltonian matrix will have the form

$$H = \begin{bmatrix} H_{11} & H_{12} \\ H_{21} & H_{22} \end{bmatrix} = \begin{bmatrix} H_{11}(|t|) & V_0 e^{-B^2|t|} \\ V_0 e^{-B^2|t|} & H_{11}(|t|) - |\Delta| \end{bmatrix}$$

and the levels will behave as in Fig 16. For $t = \pm\infty$ the adiabatic levels will coincide with the diabatic ones (a with 1 and b with 2); the model moreover assumes $|V_0| \gg |\Delta|$ so that at $t = 0$ the adiabatic levels will be approximately $H_{11}(|t|) - |\Delta|/2 \pm |V_0|$ (the + sign for level a) and the corresponding states symmetric (state a) and antisymmetric (state b) combinations of the two diabatic ones. For a complete pulse (t going from $-\infty$ to $+\infty$) the transition probability between the two states is

$$P^{(2)}_{a->b} = [sin(2V_0/\hbar B^2)/cosh(\pi\Delta/2\hbar B^2)]^2 \tag{C1}$$

The model assumes an infinite pulse time, on the other hand the result above can be thought to give an approximate transition probability for actual finite pulses; for this it is convenient to rewrite it in a more general form. V_0 represents the maximum value H_{12}^{max} reached by the interaction term H_{12} at the peak of the pulse; B^2 can instead be written as $|dH_{12}/dt|/H_{12}$. Since nonadiabatic transitions are expected to take place when $H_{12} \approx |\Delta|$ (that is when the separation of the adiabatic levels is about twice the separation $|\Delta|$ of the diabatic ones) [51], to apply the model to a case where $|dH_{12}/dt|$ is not a constant, our best choice will be to calculate B^2 when $H_{12} = |\Delta|$. A classical resonance zone in phase space that is not only always present in a certain region but also keeps growing with increasing values of the perturbation parameter, can manifest itself in a Demkov-like interaction of quantum levels [52]. The Demkov model can therefore be useful when dealing with two level interactions related to classical primary resonances.

APPENDIX D: SCALING [22]

Figure 17.a shows, the experimental peak microwave field strength for 10% ionization $F_0(10\%)$ vs. ω_0', in the region $\omega_0' \approx 1$ extended beyond the central peak of classical stability due to trapping of the ensemble within the principal primary resonance island. We observe a gradual increase of $F_0(10\%)$, very clear for decreasing frequencies and less so on the high frequency side. This lack of clarity is partly due to the big step we encounter between the $n_0 = 72$ and the $n_0 = 80$ data: to keep the ionization cutoff in n (usually around $n = 90$ for $n_0 = 65, 69, 72$) far enough from n_0, the static field was changed from 8 V/cm to 1 V/cm in the $n_0 = 80$ experiments (so that the ionization cutoff is moved to $n \simeq 150$). Adapting to the present case the suggestion of mixed units advanced in ref. [53] Figure 17.b replots the data as follows: the frequency is still rescaled to n_0, but the field strength is rescaled to the action at the center of the resonance and corrected to the first order for the static field $F_r' = F_r(1 + 7F_{rS})$ [14]. The data now connect reasonably well but since the new vertical scale is stretched with respect to F_0 for $\omega_0' < 1$ and compressed for $\omega_0' > 1$ (and increasingly so the further we move away from $\omega_0' = 1$), it progressively flattens the ionization threshold structures the higher the values ω_0' at which they appear. Finally we note that if ω_0' is changed by changing n_0 (as it is the case in ref. [53]), then the ratio between F and F_r' is constant; if ω_0' is instead changed by changing ω itself (as it is the case for each of the four series of data in Fig. 17), it is the ratio between F and F_0 that remains constant.

[1] E. Schrodinger, Naturwissenschaften **28**, 664 (1926).
[2] H.A.Lorentz *in Letters on Wave Mechanics*, K. Przibram ed. (Philosophical Library, New York, 1967).
[3] For a review of the construction of such packets in atomic systems see: I.Sh Averbukh and N.F. Perel'man, Sov. Phys. Usp. **34**, 572 (1991).
[4] A. Buchleitner, These de Doctorat de l'Université Pierre et Marie Curie, Paris 6 (1993);D. Delande and A. Buchleitner, *Adv. At. Mol. and Opt. Phys.*, **34**, 85 (1994), and D. Delande, J. Zakrzewski and A. Buchleitner, Europhys. Lett. **32**, 107 (1995).
[5] I. Bialynicki-Birula, M. Kalinski and J.H. Eberly, Phys. Rev. Lett. 73, 1777 (1994).
[6] A. Buchleitner and D. Delande, Phys. Rev. Lett. 75, 1487 (1995). J. Zakrzewski, D. Delande and A. Buchleitner, Phys. Rev. Lett. **75**, 4015 (1995).
[7] See e.g. A. Buchleitner, D. Delande, and J. Zakrzewski, Phys. Rep. **368**, 409 (2002) and references therein.
[8] See e.g. F. B. Dunning , J. J. Mestayer1 , C. O. Reinhold , S. Yoshida, and J. Burgdoerfer, J. Phys. B **42**, 022001 (2009); H. Maeda and T. F. Gallagher, Phys. Rev.**A75**, 033410 (2007) and references therein.
[9] G. Radons and R. E. Prange, Phys. Rev. Lett. **61**, 1691 (1988).
[10] K. Dietz, J. Henkel and M. Holthaus, Phys. Rev. **A45**, 4960 (1992).
[11] E.J. Heller, Phys. Rev. Lett. **53**, 1515 (1984).
[12] Y.-C. Lai, C. Grebogi, R. Blumel and M. Ding, Phys. Rev. **A45**, 8284 (1992).
[13] R.V. Jensen, M.M. Sanders, M. Saraceno and B. Sundaram, Phys. Rev. Lett. **63**, 2771 (1989).
[14] L. Perotti, "Small Phase Space Structures and their Relevance to Pulsed Quantum Evolution: the Stepwise Ionization of the Excited Hydrogen Atom in a Microwave Pulse", To be submitted to Phy. Rev. A. arXiv:0906.5180v1
[15] I have shown it analytically only in pendulum approximation [14] (see appendix A for a breaf description of it); but a direct measurement of the distances between the (numerically calculated) quasienergy levels of the principal primary quantum nonlinear resonance shows that they are equally spaced also for the full problem.
[16] Similarly, in the same limit, states with $k \gtrsim 0$ are essentially excited harmonic oscillator states forced to oscillate at the microwave frequency (see ref. [10]).
[17] E.V. Shuryak; Sov. Phys. JETP **44**, 1070 (1976).
[18] R.S. Mackay, J.D. Meiss and I.C. Percival, Physica **D27**, 1 (1987).
[19] L. Sirko, M.R.W. Bellermann, A. Haffmans, P.M. Koch and D. Richards, Phys. Rev. Lett. **71**, 2895 (1993).
[20] J.G. Leopold and D. Richards, J. Phys. **B27**, 2169 (1994).
[21] P.M. Koch, Physica **D83**, 178 (1995).

[22] L. Perotti; Ph. D. Thesis, Un. of Pittsburgh (1996)
[23] H.P. Breuer, K. Dietz and M. Holthaus, Z. Phys. **D18**, 239 (1991).
[24] J.E. Bayfield, S.Y. Luie, L.C. Perotti and M.P. Skrzypkovski, Phys. Rev. **A53**, R12 (1996).
[25] R. V. Jensen, M. M. Susskind and M. M. Sanders, Phys. Rep. **201**, 1 (1991).
[26] G. Casati, B.V. Chirikov, D.L. Shepelyansky and I. Guarneri; Phys. Rep. **154**, 77 (1987).
[27] Damburg and Kolosov in *Rydberg states of atoms and molecules* ,R.F. Stebbings and F.B. Dunning eds., Cambridge (1983).
[28] G. Casati and L. Molinari, Suppl. Progr. Theor. Phys. **98**, 287 (1989).
[29] H.P. Breuer, K. Dietz and M. Holthaus, J. Phys. **B22**, 3187 (1989).
[30] J. Von Neumann and E. Wigner, Phys. Z. **3**, 467 (1929).
[31] H.P. Breuer and M. Holthaus, Z. Phys. **D11**, 1 (1989).
[32] For a discussion of the problems connected to basis truncation in the calculation of quasienergies and in the definition of an adiabatic limit see D. W. Hone, R. Ketzmerick and W. Kohn, Phys. Rev. **A56**, 4045 (1997).
[33] K. Husimi, Proc. Phys. Math. Soc. Jpn. **22**, 264 (1946).
[34] G.P. Berman and G.M. Zaslavsky, Phys. Lett. **A61**, 295 (1977).
[35] K. Dietz, J. Henkel and M. Holthaus, Phys. Rev. **A45**, 4960 (1992).
[36] G. Casati, I. Guarneri and D.L. Shepelyansky, Phys. Rev. **A36**, 3501 (1987).
[37] In the case of a chaotic separatrix band, the classical motion stops being periodic altogether. On the other hand, motion along the manifolds of the unstable fixed point still becomes infinitely slow when approaching the fixed point. Moreover, even in the case of a fairly wide chaotic band as in Fig. 3, the points of the ensemble appear (for slow switch-on times) to approach the unstable fixed point along the stable manifold and bunch-up close to the fixed point before shooting off along the unstable manifold.
[38] G.P. Berman and A.R. Kolovskii, Sov. Phys. Usp. **35**, 303 (1992).
[39] To find n_s we first calculate the resonant action I_r; n_s is then the integer closest to $2I_r - n_0$. Since I_r is calculated making use of the approximate formula $\omega I_r^3/(1-3F_S I_r^4) = 1$, in same cases the n_s thus calculated can be off by one; we therefore always numerically calculate the zero microwave field quasienergies for n_s, n_s+1 and n_s-1; the real n_s is the one of these whose quasienergy is closest to that of n_0.
[40] In particular, in the cases when other peaks are present, the quantum final population on the peak centered at n_0 displays oscillations as a function of F^{max} that are absent from the corresponding classical simulations. The absence of classical oscillations is due to the scrambling of the phases induced by the chaotic band (using the integrable pendulum approximation and parameters comparable to the present ones, oscillations are present [35]); their presence in the quantum simulation seems to indicate that the quantum system is at least partially blind to the chaotic band at the separatrix. The scarring itself of the separatrix FE can be interpreted as expression of this blindness [54].
[41] E.J. Heller, J. Phys. Chem. **99**, 2625 (1995).
[42] A similar indifference of the quantum system to chaotic bands and agreement with the behaviour expected from just the resonant term has been observed in other models: see e.g. ref. [54].
[43] The initial decay of about 80% in the population of this state and of about 20% of the $n = 65$ state it is "crossing" happens in less than one microwave period; afterwards both states decay at the same rate.
[44] G. Casati, I. Guarneri and D.L. Shepelyansky, IEEE J. Quantum Electronics **24**, 1420 (1988).
[45] M.J. Stevens and B. Sundaram, Phys. Rev. **A36**, 417 (1987).
[46] M. Abramowitz and I.A. Stegun, *Handbook of mathematical functions*, Dover Publ. New York (1964).
[47] D. Richards, in *classical Dynamics in atomic and molecular physics*, T. Grozdanov, P. Grujic and P. Krstic Eds., World Scientific, Singapore (1989)
[48] L. Sirko and P.M. Koch, Appl. Phys.**B60**, S195 (1995).
[49] I.S. Gradshtenyn and I.M. Ryzhik, *Table of Integrals, Series, and Products*, Academic Press (1980).
[50] Actually, for an orbit within the resonance zone, both $\langle x\rangle$ and $\langle\varphi\rangle$ are zero in pendulum approximation. This means that the average position of the orbit is at the center of the resonance zone, that is: it coincides with the point representing in sectioned phase space the stable periodic orbit. Quantization of the tori within the resonance zone will therefore result in eigenfunctions centered on that same orbit and oscillating in phase with it.
[51] Ju.N. Demkov, "Charge Exchange with Small Energy Transfer", in *Atomic Collision Processes*, M.R.C. Mc Dowell Ed., North-Holland Amsterdam (1964).
[52] A simple example is in this case the pendulum Hamiltonian $H = H_0 + V$ where $V = 2V_0\lambda cos(\varphi)$, $H_0 = A[I-(|\Delta|/A-1)/2)^2$ and we assume $\lambda = e^{-B^2|t|}$. If we take $|\Delta| \approx 2A$ and we perform the usual "semiclassical" quantization $I = -i\partial/\partial\varphi$ on the base $|m>= e^{im\varphi}/\sqrt{2\pi}$, the two states $|0>$ and $|1>$ will be closer to each other than to any other state interacting with them. It will therefore be possible (as long as $V_0 \ll 2A$) to treat them as a two-level system with a Hamiltonian matrix as the one given above.
[53] P.M. Koch and K.A.H. van Leewen, Phys. Rep. **255**, 289 (1995).
[54] M. Holthaus, Chaos, Solitons & Fractals **5**, 1143 (1995).

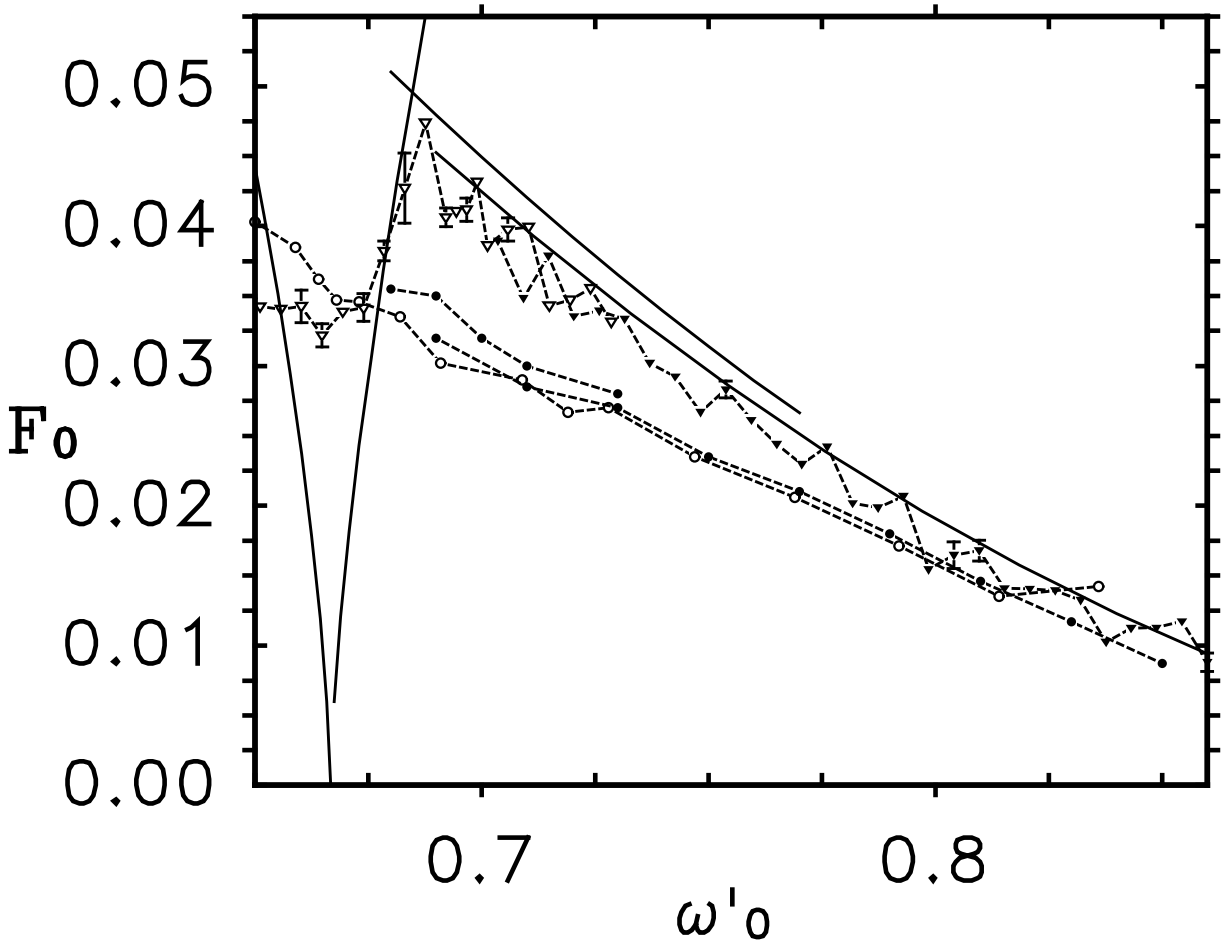

FIG. 1: Signs of quantum localization in the ionization data. Circles are the classical $F_0(10\%)$; triangles, full ($n_0 = 69$) and empty ($n_0 = 65$), the experimental one. Heavy curves: evaluation of the separatrix action location from eq. A2; the "V" on the left is for the $\omega_0' = 2/3$ resonance zone, the two curves on the right are for the principal primary resonance zone, for the two cases $n_0 = 65$, $F_S = 8$ V/cm (upper curve)and $n_0 = 69$, $F_S = 8$ V/cm (lower curve). The experimental data for $\omega_0' > 0.7$ are higher than the classical ones and show reasonable agreement with the pendulum approximation separatrix location curves. The full dots mark the fields at which classical ensembles with initial conditions at various values of ω_0' enter the primary resonance zone. (From Ref. [22])

.

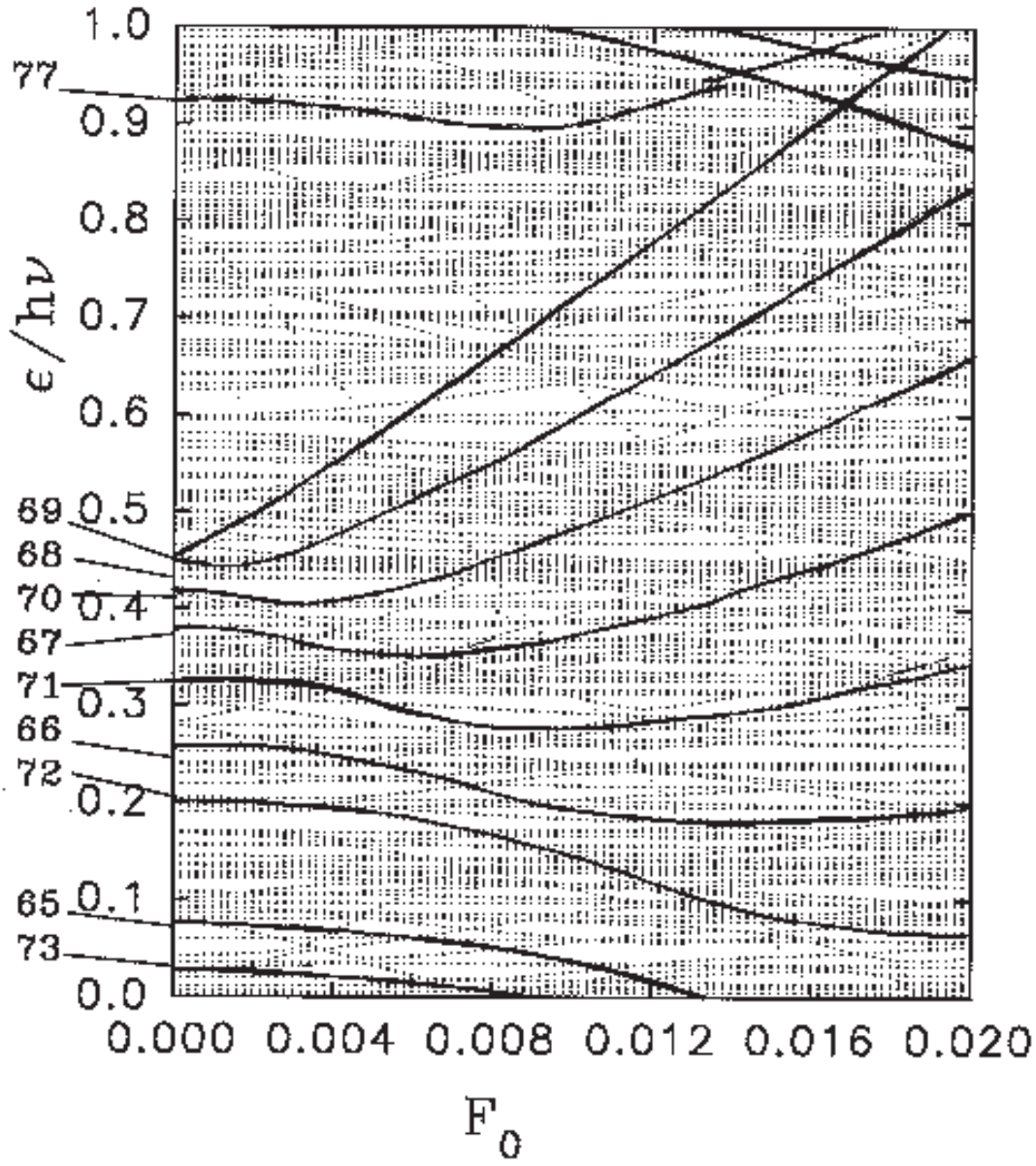

FIG. 2: Quasienergy curves for the rescaled (to $n_0 = 65$) parameters $\omega_0' = 0.8196$ and $F_{0S} = 0.02777$; the horizontal scale is the rescaled microwave field strength. The curves of the levels belonging to the $\omega_0' = 1/1$ nonlinear quantum resonance are marked as darker lines; the dashed line is the $n = 77$ level, having an avoided crossing with $n_0 = 65$ for $F_0 \simeq 0.016$.

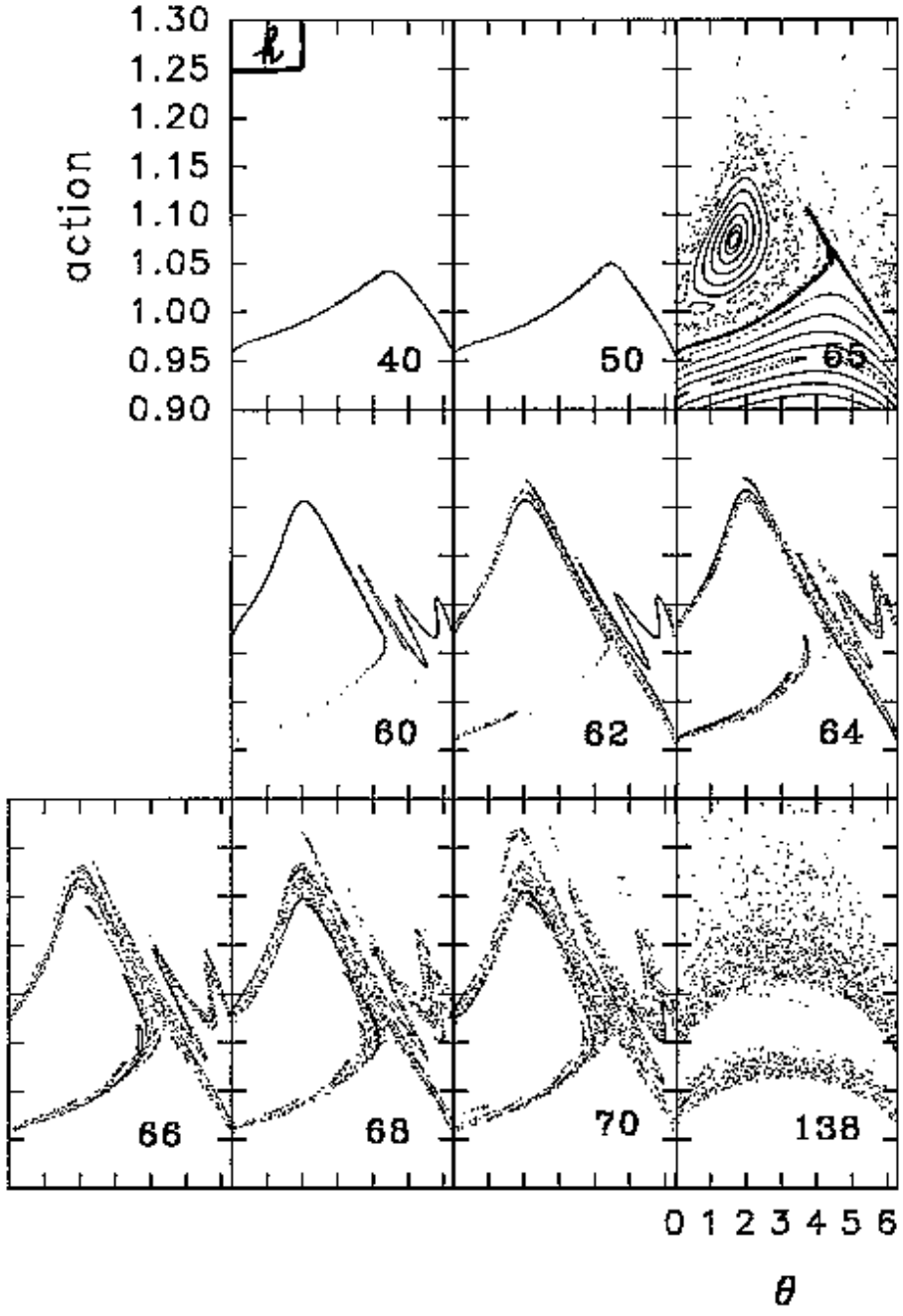

FIG. 3: Classical ensemble at different times (indicated for each snapshot) during the rise of the microwave pulse and at the end of it. The parameters are: $\omega_0' = 0.8196$, $F_0^{max} = 0.01607$, $F_{0S} = 0.02777$, $T = 140$ microwave periods. The size of Planck's constant h for $n_0 = 65$ is indicated. The instantaneous surface of section at the crossing time is shown, displaying a wide chaotic separatrix region. (From Ref. [22])

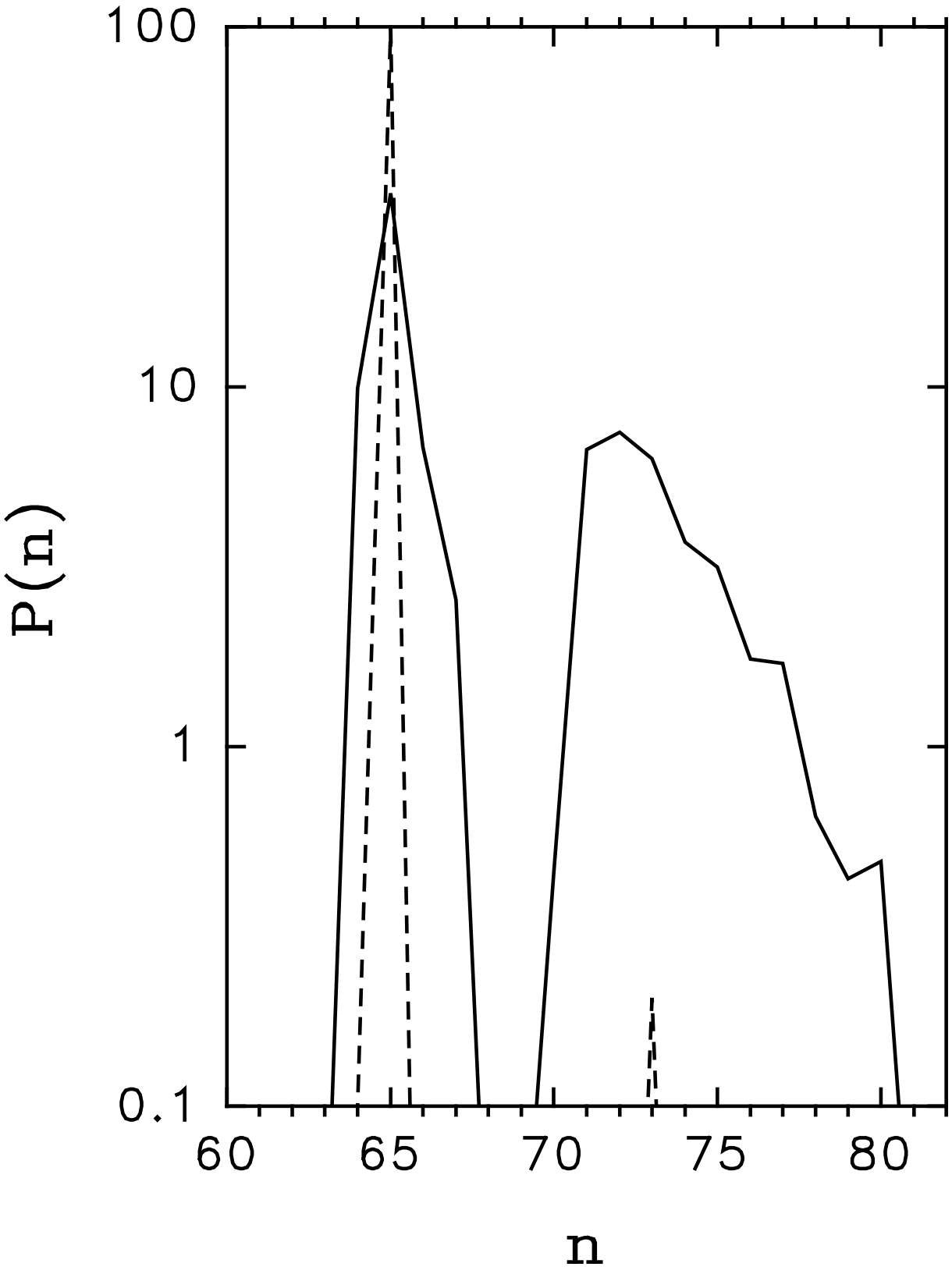

FIG. 4: Classical (full line) and quantum (dashed line) final n-distribution for the parameters $\omega_0' = 0.8196$, $F_0^{max} = 0.01607$, $F_{0S} = 0.02777$, $T = 140$ microwave periods and $n_0 = 65$. The return of most of the quantum population to $n_0 = 65$ suggests an (almost) adiabatic evolution. (From Ref. [22])

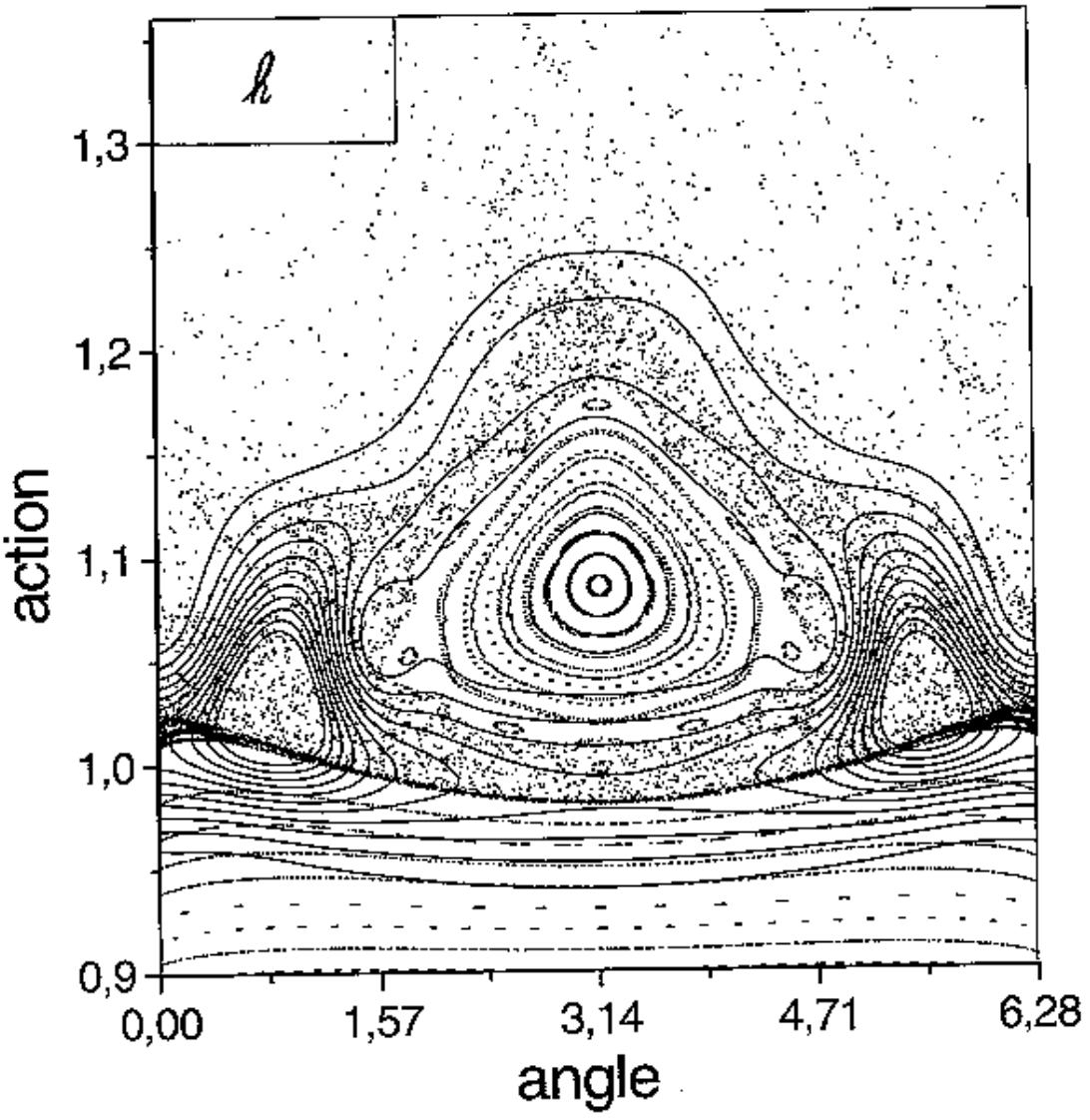

FIG. 5: Husimi function of the quantum wavefunction at the peak of the pulse. The parameters are still $\omega_0' = 0.8196$, $F_0^{max} = 0.01607$, $F_{0S} = 0.02777$, $T = 140$ microwave periods and $n_0 = 65$. For comparison the classical instantaneous surface of section is also shown. As suggested by the symmetric shape of the Husimi function and its adherence to the outlines of the classical surface of section, the wavefunction is almost completely a single Floquet eigenstate.

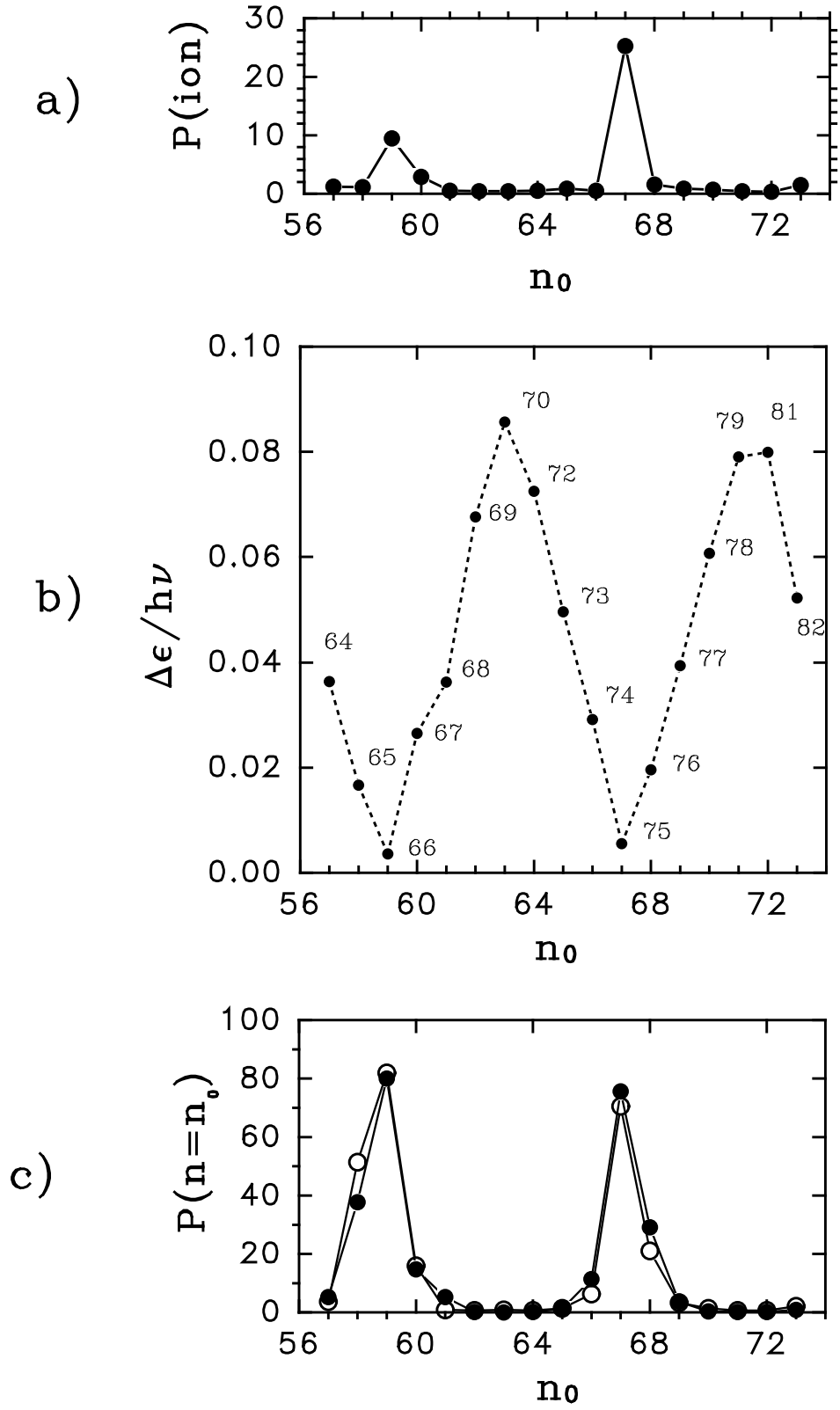

FIG. 6: a) Quantum ionization probability versus initial Stark quantum number n_0. b) Zero microwave field quasienergy difference between the initial quantum Stark state n_0 and n_s (indicated for every point) versus n_0. c) fitting of the Demkov model (full circles) to the numerically calculated population that has left n_0 at the end of the pulse (open circles). The parameters are: $\omega_0' = 0.8196$, $F_0^{max} = 0.01607$ and $F_{0S} = 0.02777$. Local maxima in a) and c) correspond to minima in b) indicating the connection of (semiclassical) nonadiabatic evolution with two level quantum resonances. (From Ref. [22])

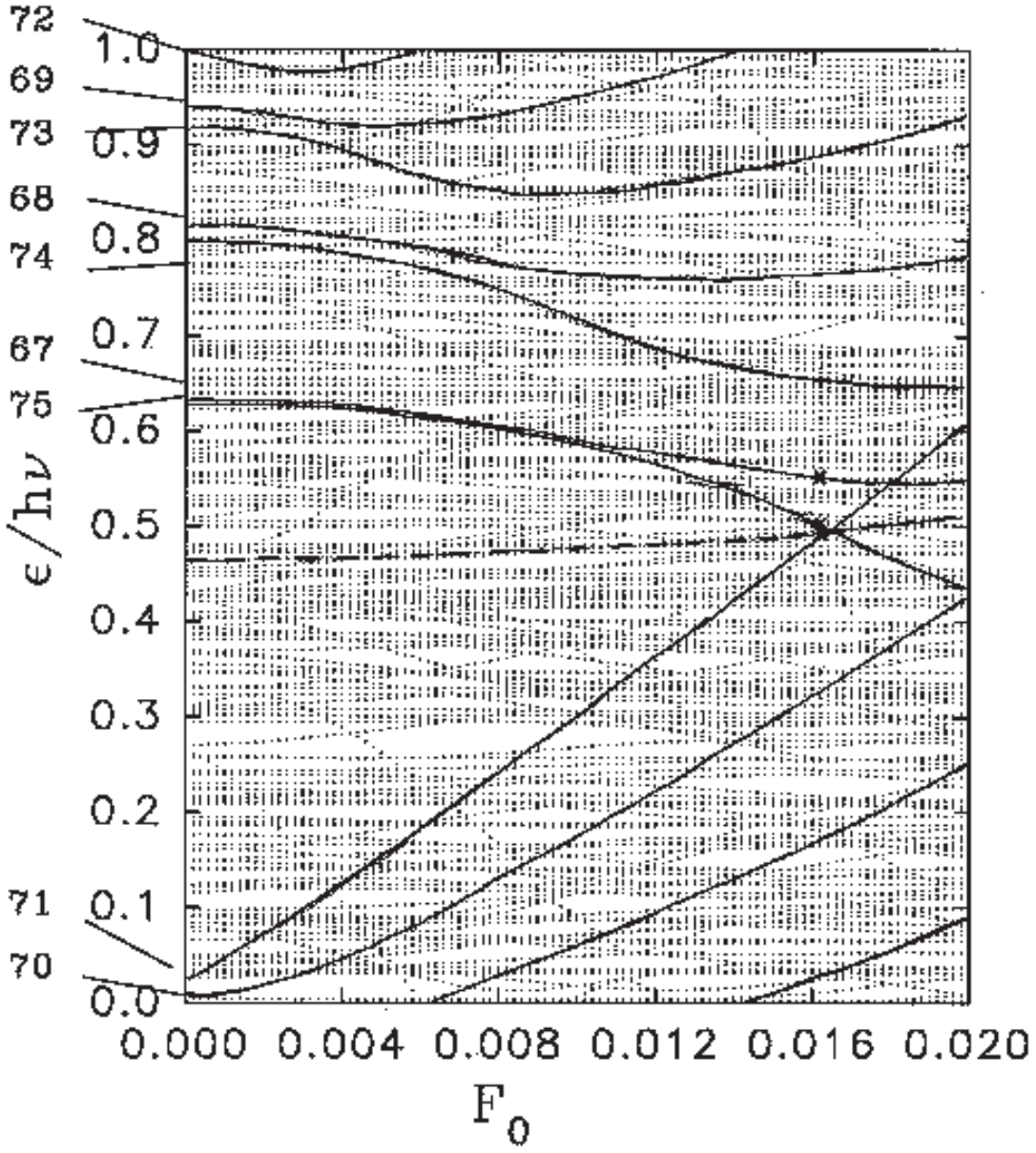

FIG. 7: Quasienergy curves for the rescaled (to $n_0 = 67$) parameters $\omega_0' = 0.8196$ and $F_{0S} = 0.02777$; the horizontal scale is the rescaled microwave field strength. The curves of the levels belonging to the $\omega_0' = 1/1$ nonlinear quantum resonance are marked as darker lines. The crosses indicate the quasienergies of the eigenstates most populated at the peak of the pulse discussed in the text: 39.1% of the population is on the $n = 67$ state and $23.4 + 16.6\%$ on the state $n = 75$ undergoing at that field value a narrow avoided crossing with a state of the second well (dashed line).

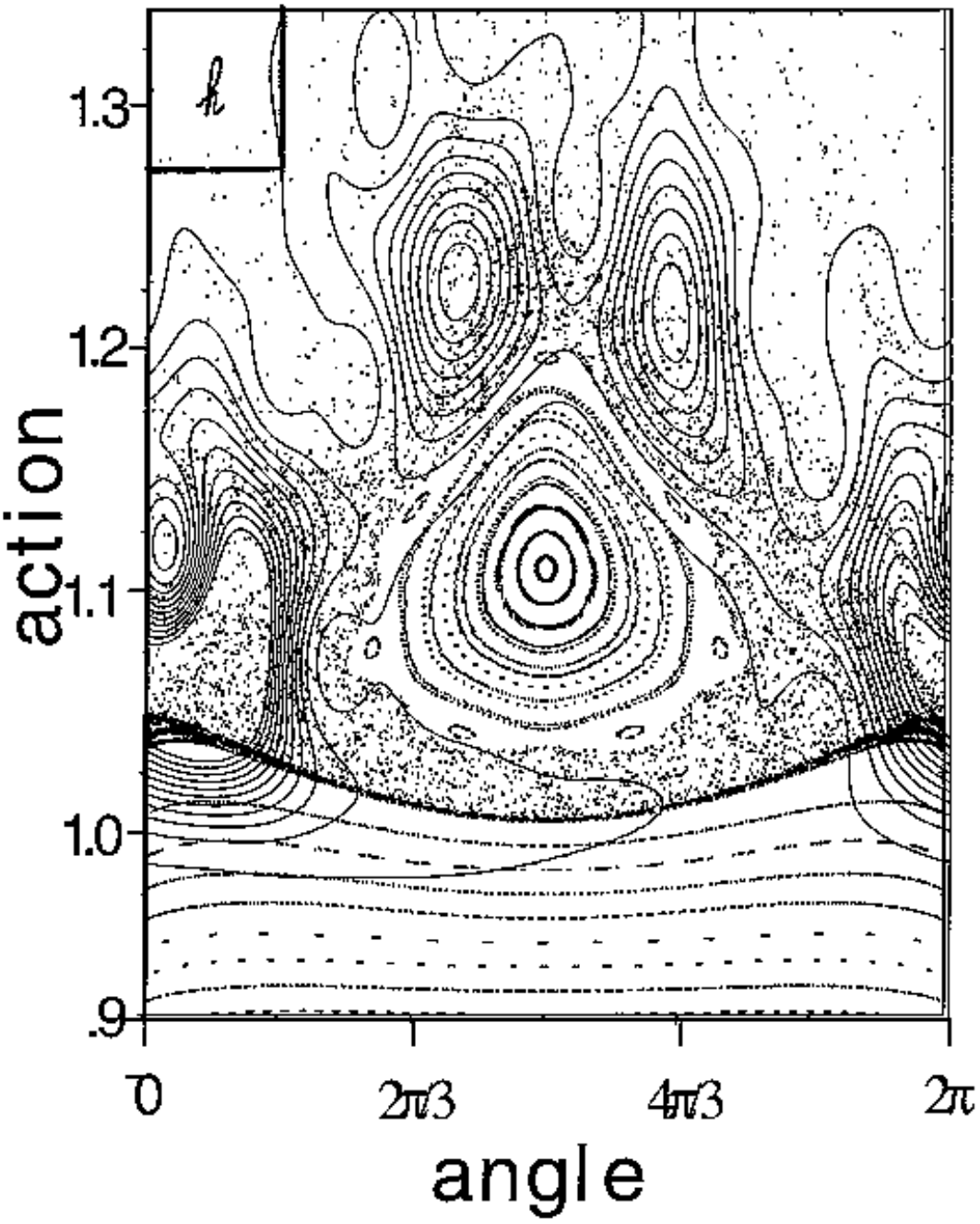
ħ
1.3
1.2
1.1
1.0
.9
action
0
2π3
4π3
2π
angle

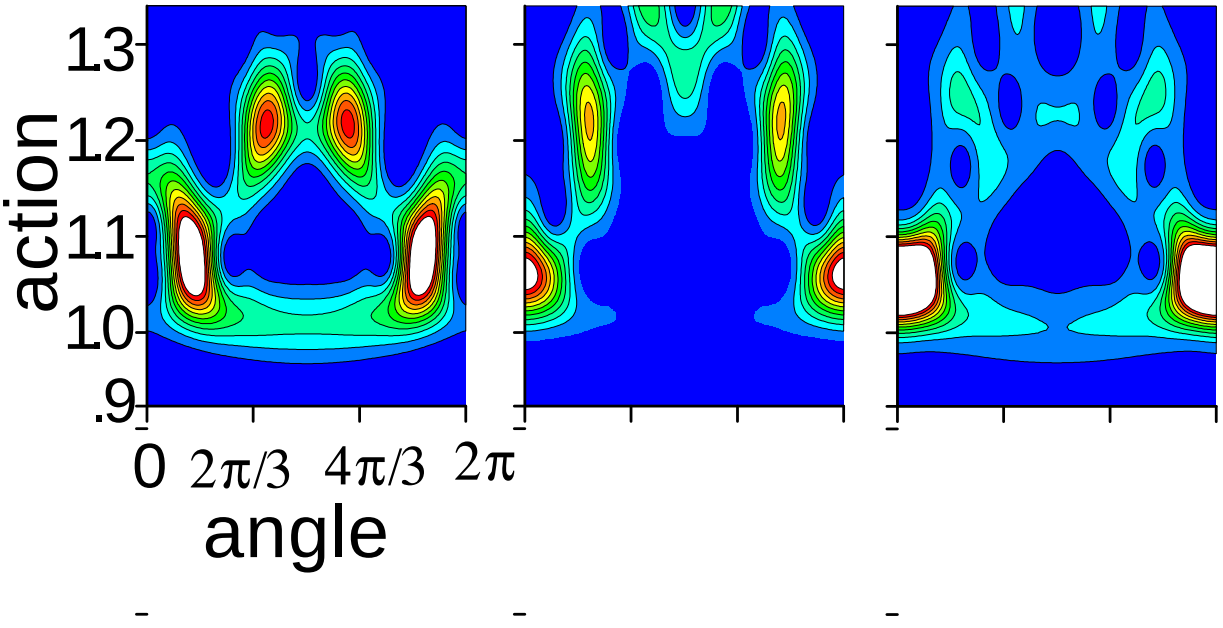

FIG. 8: a) Husimi function of the quantum wavefunction at the peak of the pulse. The parameters are $\omega_0' = 0.8196$, $F_0^{max} = 0.01607$, $F_{0S} = 0.02777$, $T = 140$ microwave periods and $n_0 = 67$. For comparison the classical instantaneous surface of section is also shown. The symmetry of Fig. 5 has been broken and the Husimi function can only losely be said to reflect the classical phase structure in its avoidance of the principal primary island at the center of the figure. b) Husimi functions of the three eigenstates on which the above instantaneous wavefunction has the highest projections. In the order: the $n_0 = 67$ state (39.1%), the $n_s = 75$ state (23.4%) and the "second well" state undergoing a narrow avoided crossing with the latter (16.6%).

.

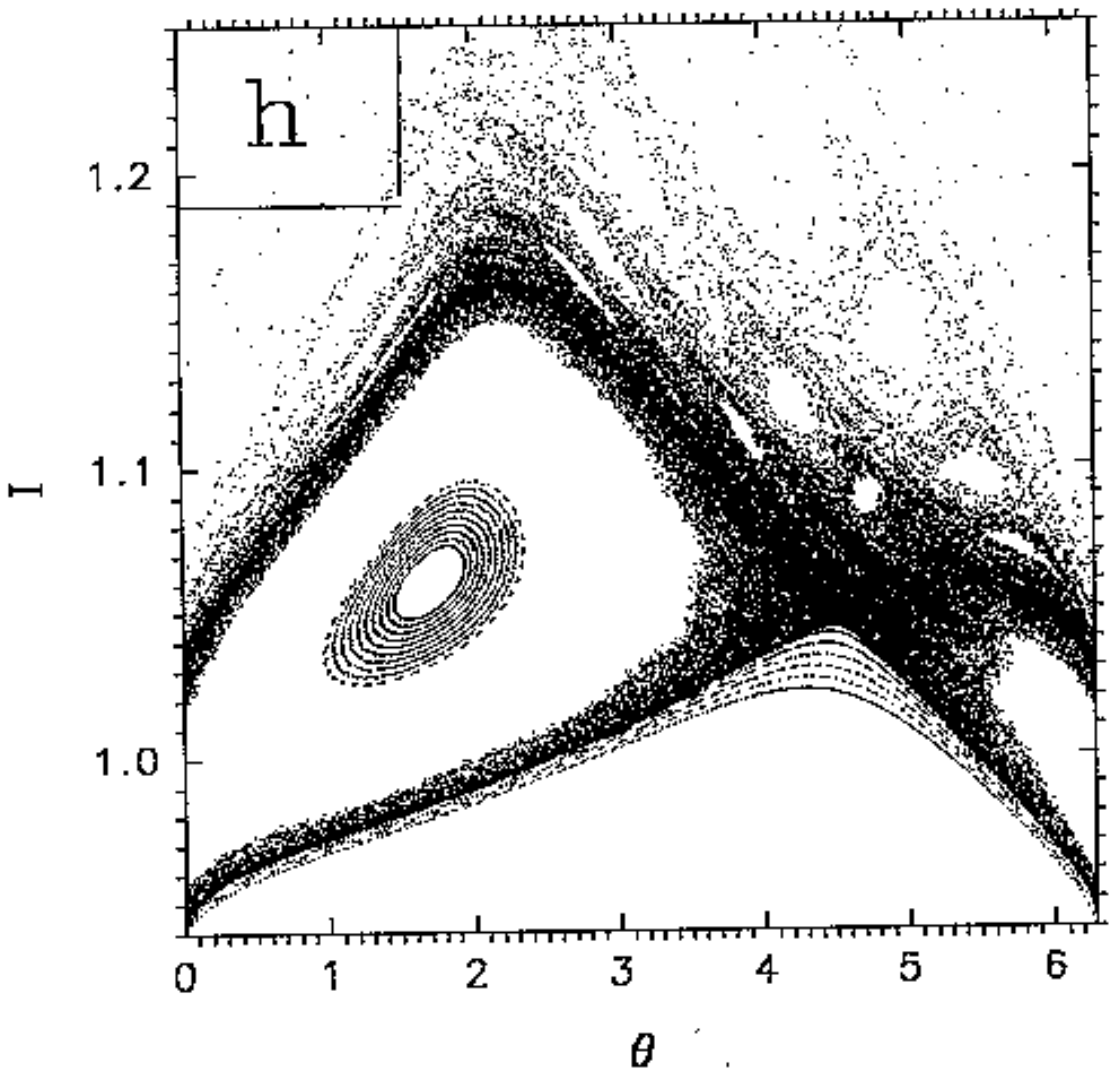

FIG. 9: Surface of section (Poincaré map) for $\omega_0' = 0.847$, $F_0 = 0.0104$, $F_{0S} = 0.035266$ and $\phi_0 = 0$. (From Ref. [22])

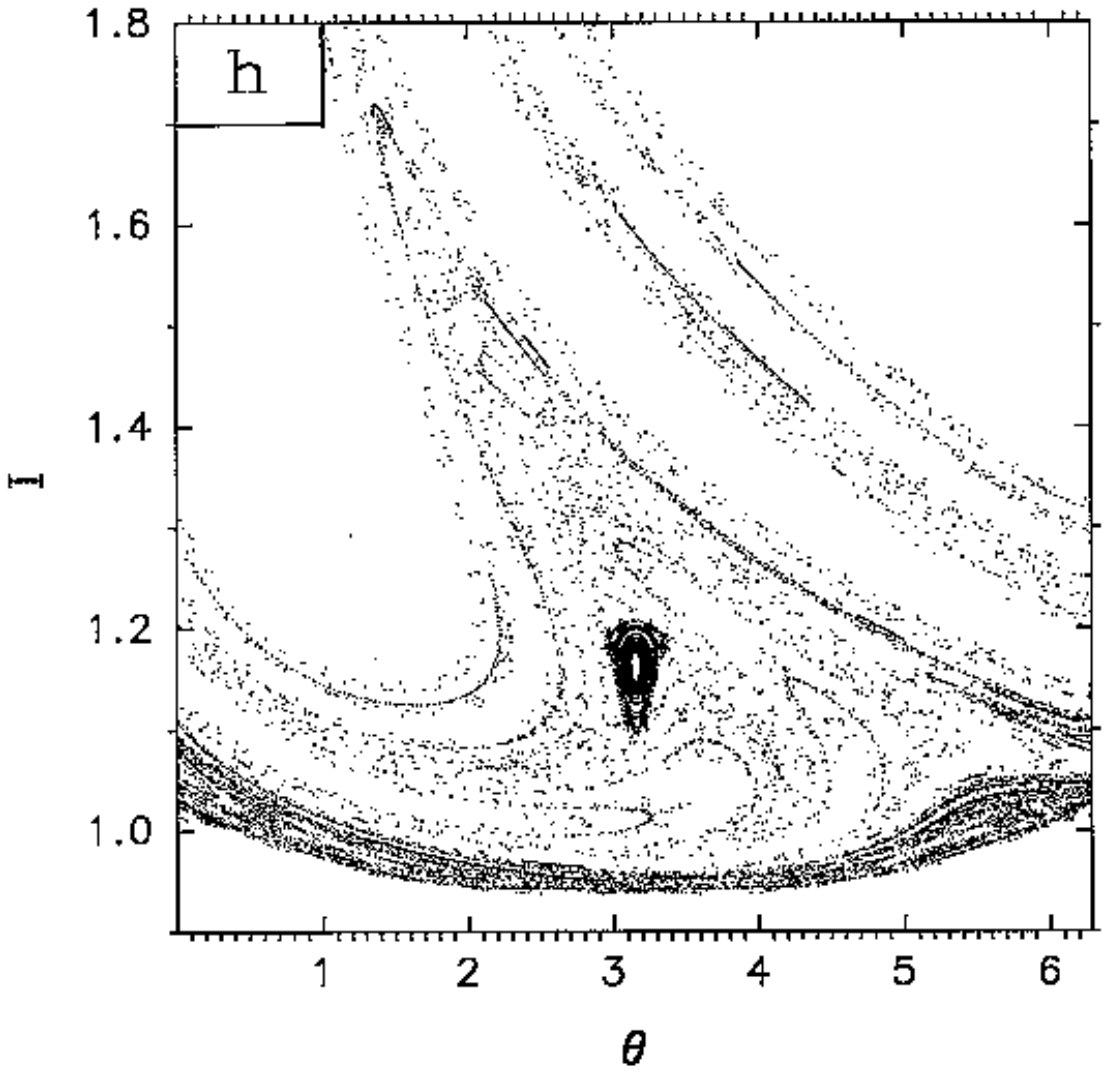
h
1.8
1.6
1.4
1.2
1.0
I
1
2
3
4
5
6
θ

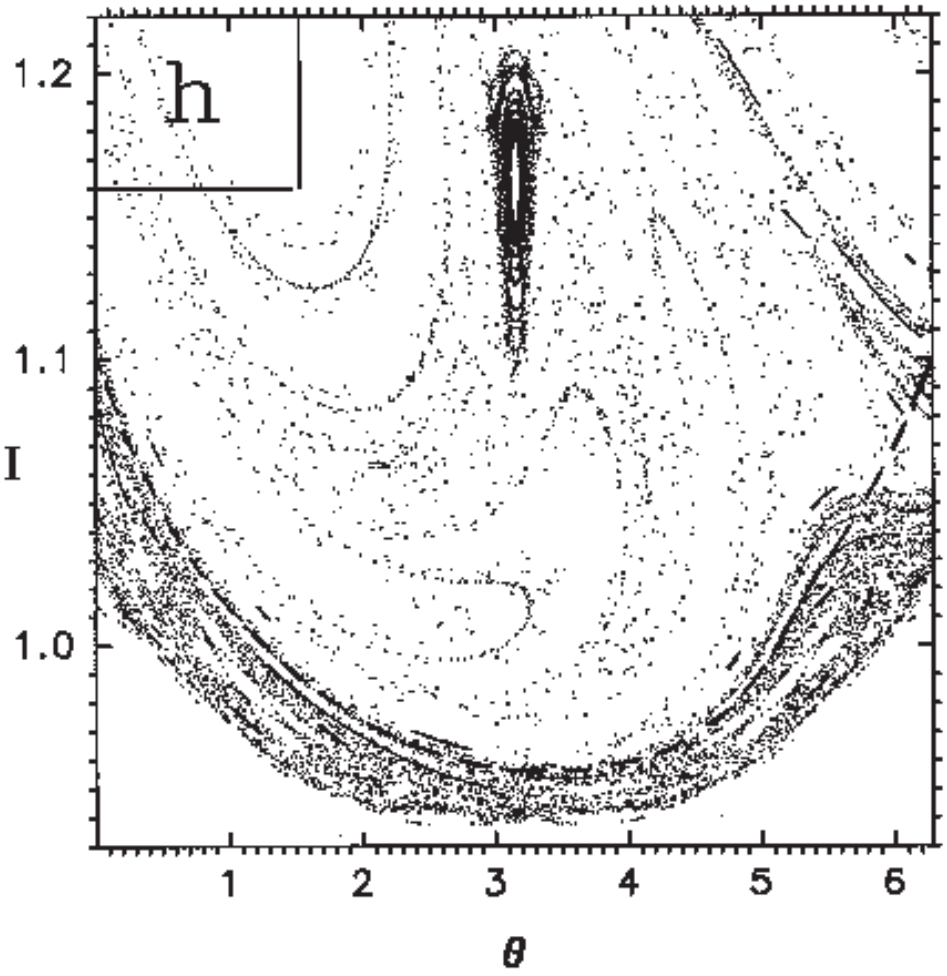

FIG. 10: a) Surface of section (Poincaré map) for $\omega_0' = 0.6876$, $F_0 = 0.045$, $F_{0S} = 0.02777$ and $\phi_0 = \pi/2$. b) detail; as in Fig. 9, the dashed line is an approximate separatrix curve.

.

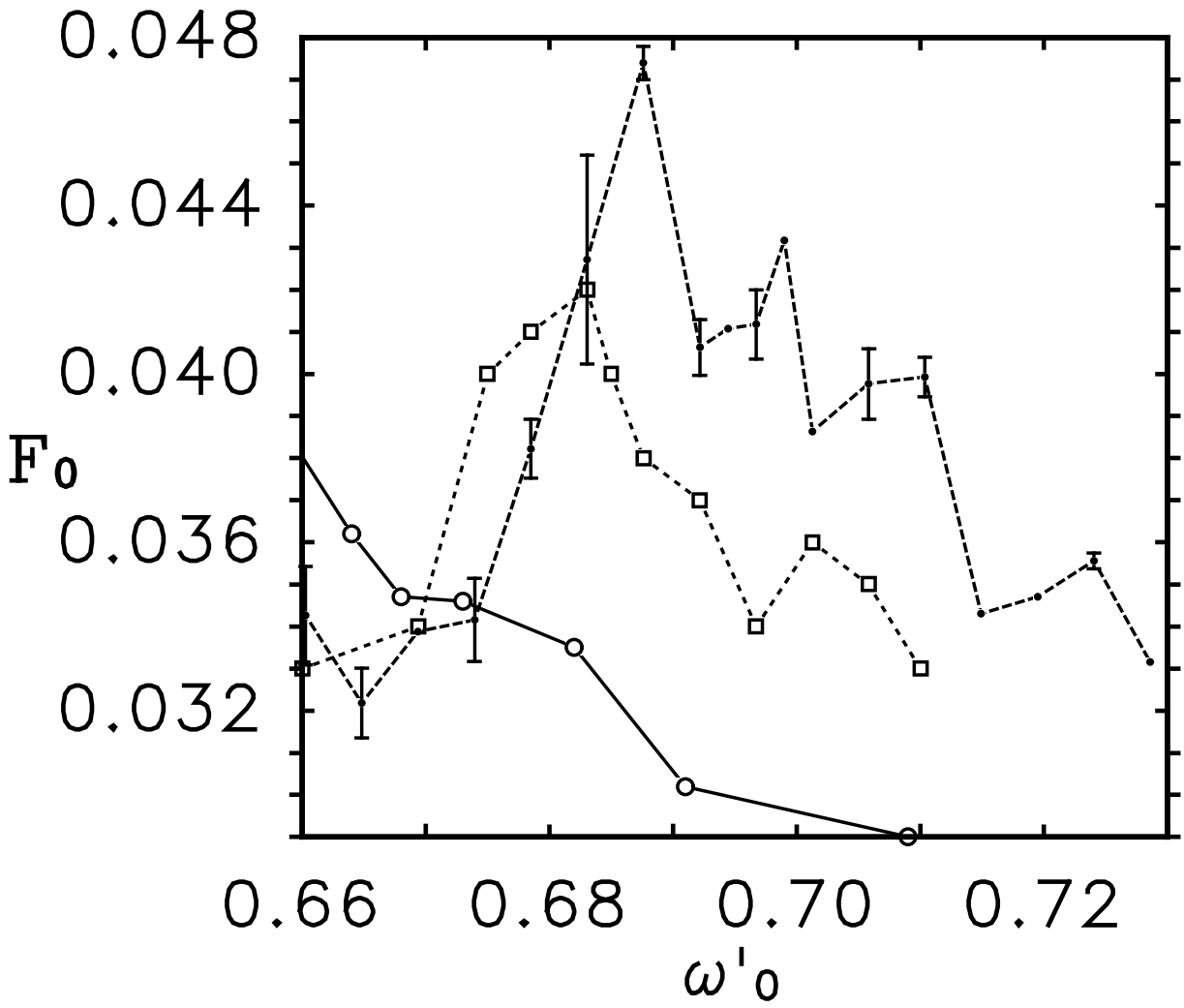

FIG. 11: Rescaled peak microwave field for 10% ionization probability $F_0(10\%)$ versus rescaled frequency ω_0'. Quantum results: squares. Experimental results: dots. Classical results: circles. The classical curve shows no sign of the quantum and experimental peak at $\omega_0' \simeq 0.68$. (From Ref. [22])

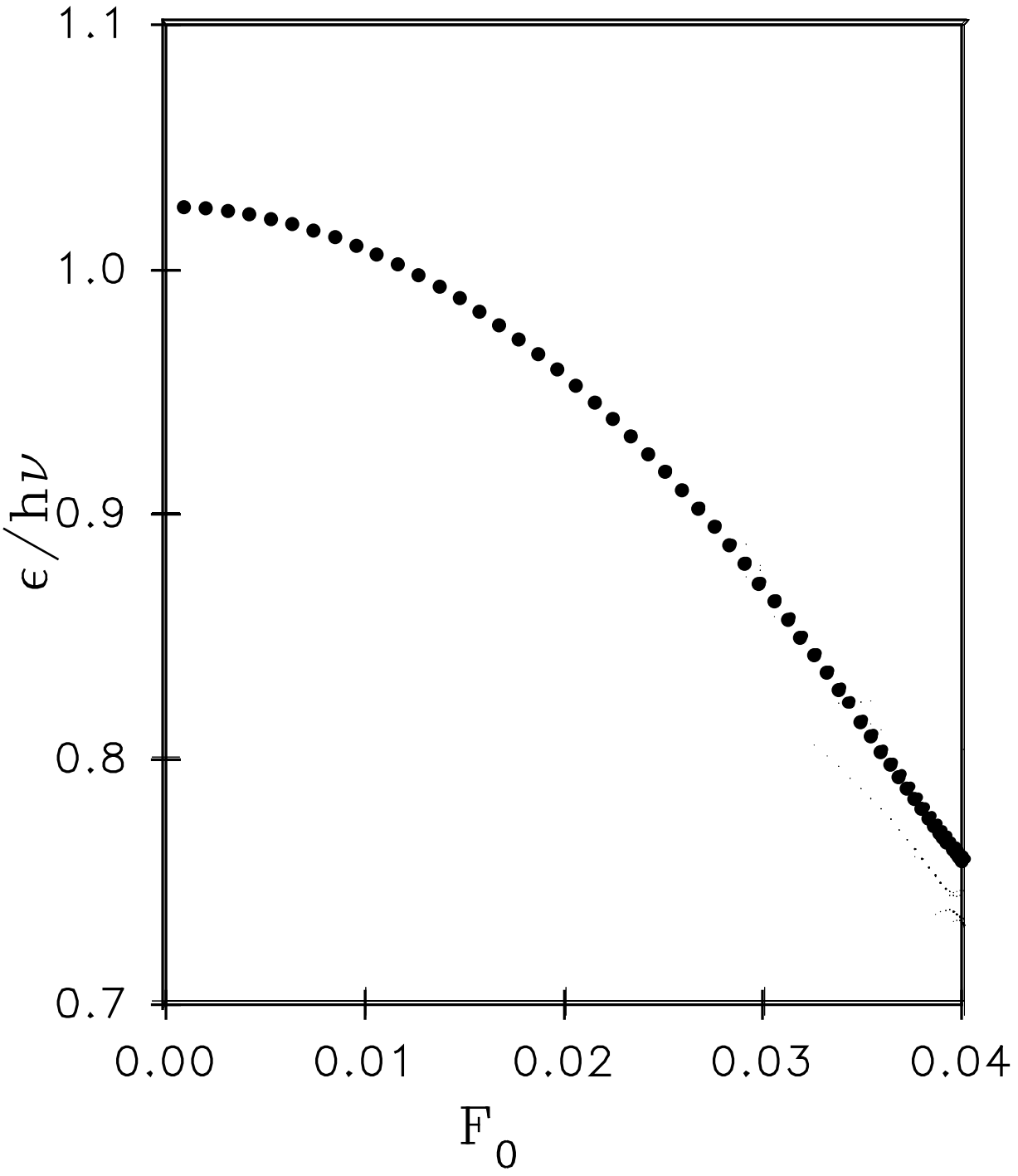
1.1
1.0
0.9
0.8
0.7
ϵ/hν
0.00
0.01
0.02
0.03
0.04
F0

.

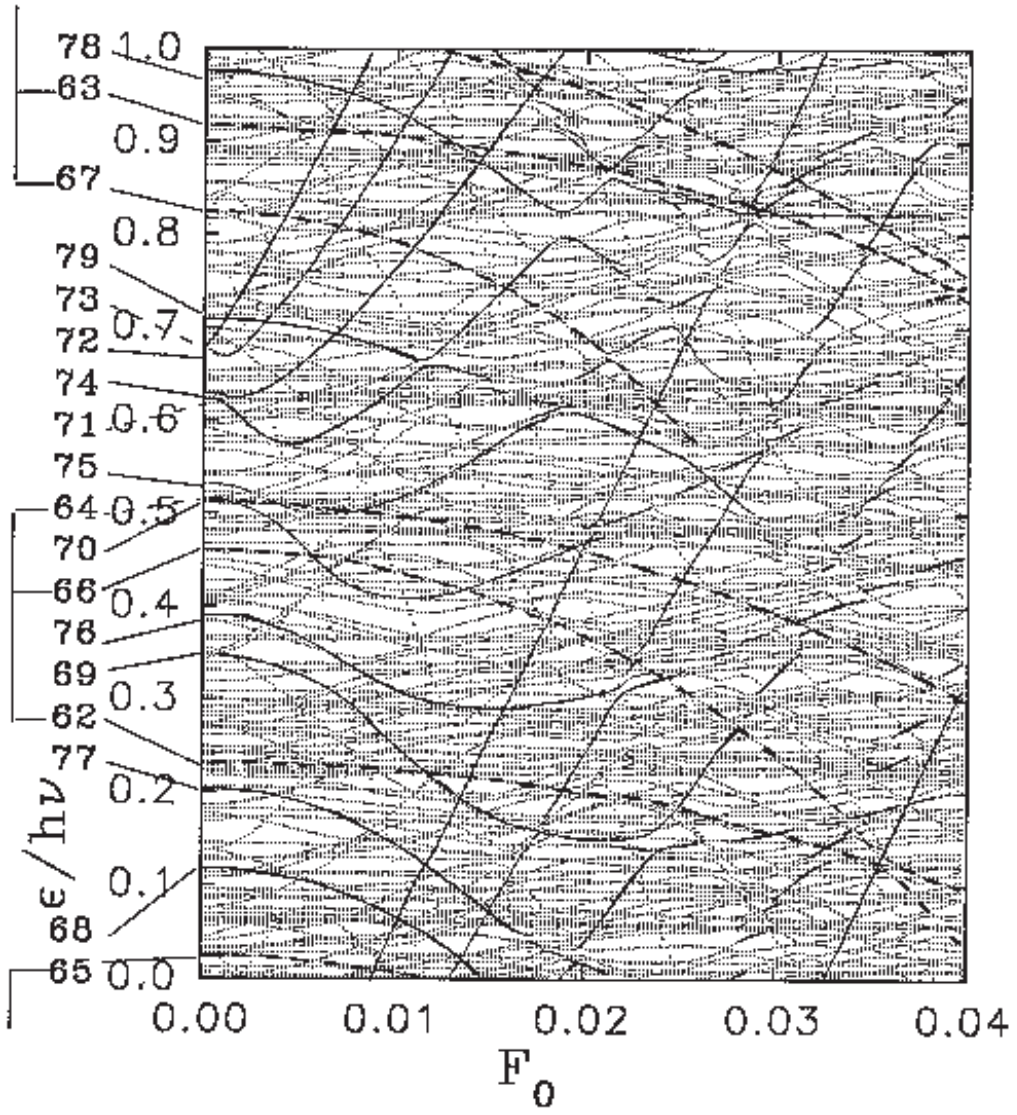

FIG. 12: a) The evolution of the projections of the wavefunction on the instantaneous Floquet states at every period of the rising edge of the microwave pulse. The parameters are: $\omega_0' = 0.675$, $F_0^{max} = 0.04$, $F_{0S} = 0.02777$, $T = 116$ microwave periods and $n_0 = 65$. The three states making up most of the probability are $n = n_0 = 65$ (full line), $n = 63$ (dashed line) and a self ionizing state (dotted line). b) Quasienergy curves for the rescaled (to $n_0 = 65$) parameters $\omega_0' = 0.675$ and $F_{0S} = 0.02777$; the horizontal scale is the rescaled microwave field strength. The curves of the levels belonging to the $\omega_0' = 1/1$ nonlinear quantum resonance are marked as full lines; the two groupings of those belonging to the $\omega_0' = 2/3$ nonlinear quantum resonance as dashed lines.

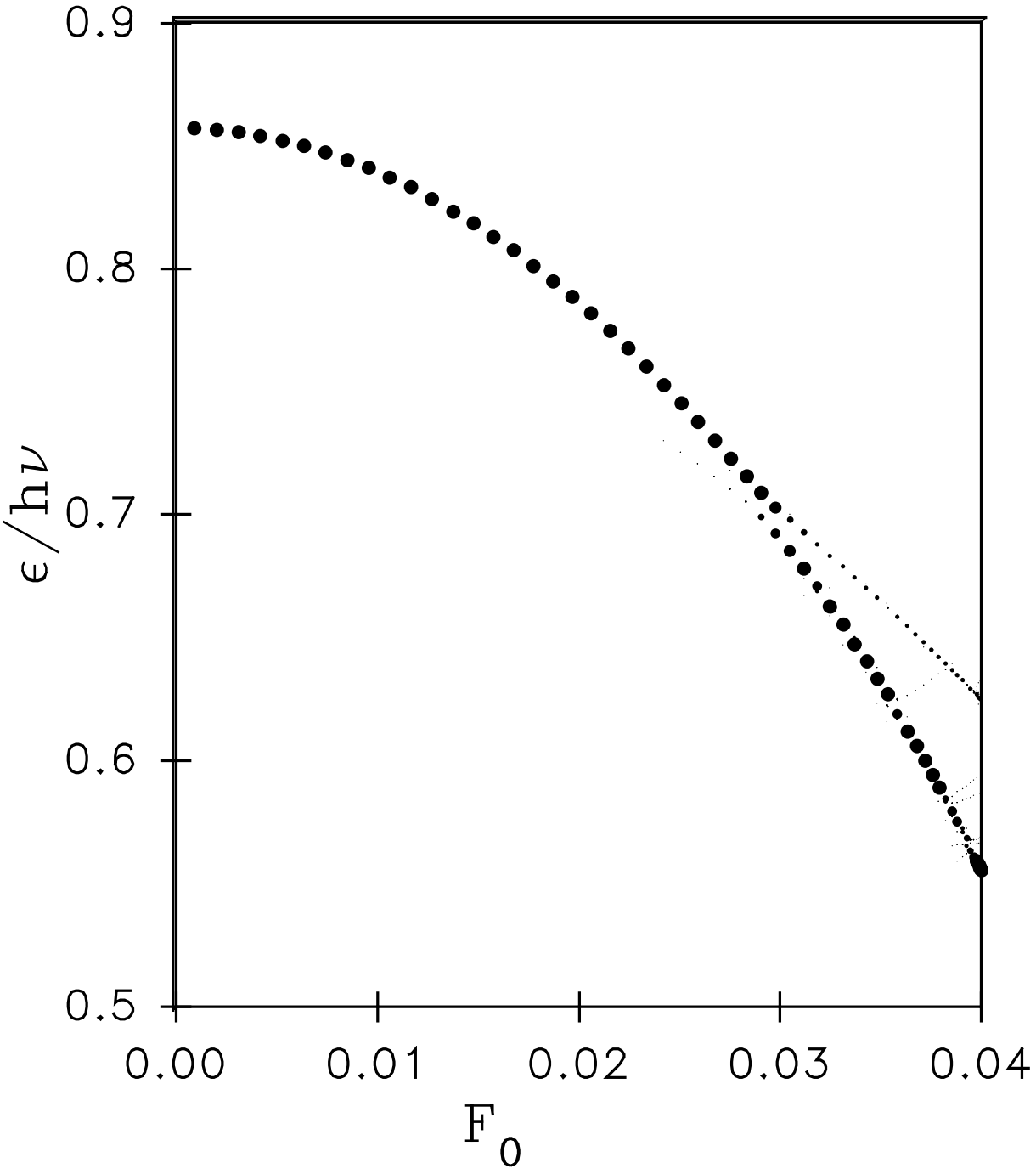
0.9
0.8
0.7
0.6
0.5
$\epsilon/h\nu$
0.00
0.01
0.02
0.03
0.04
F_0

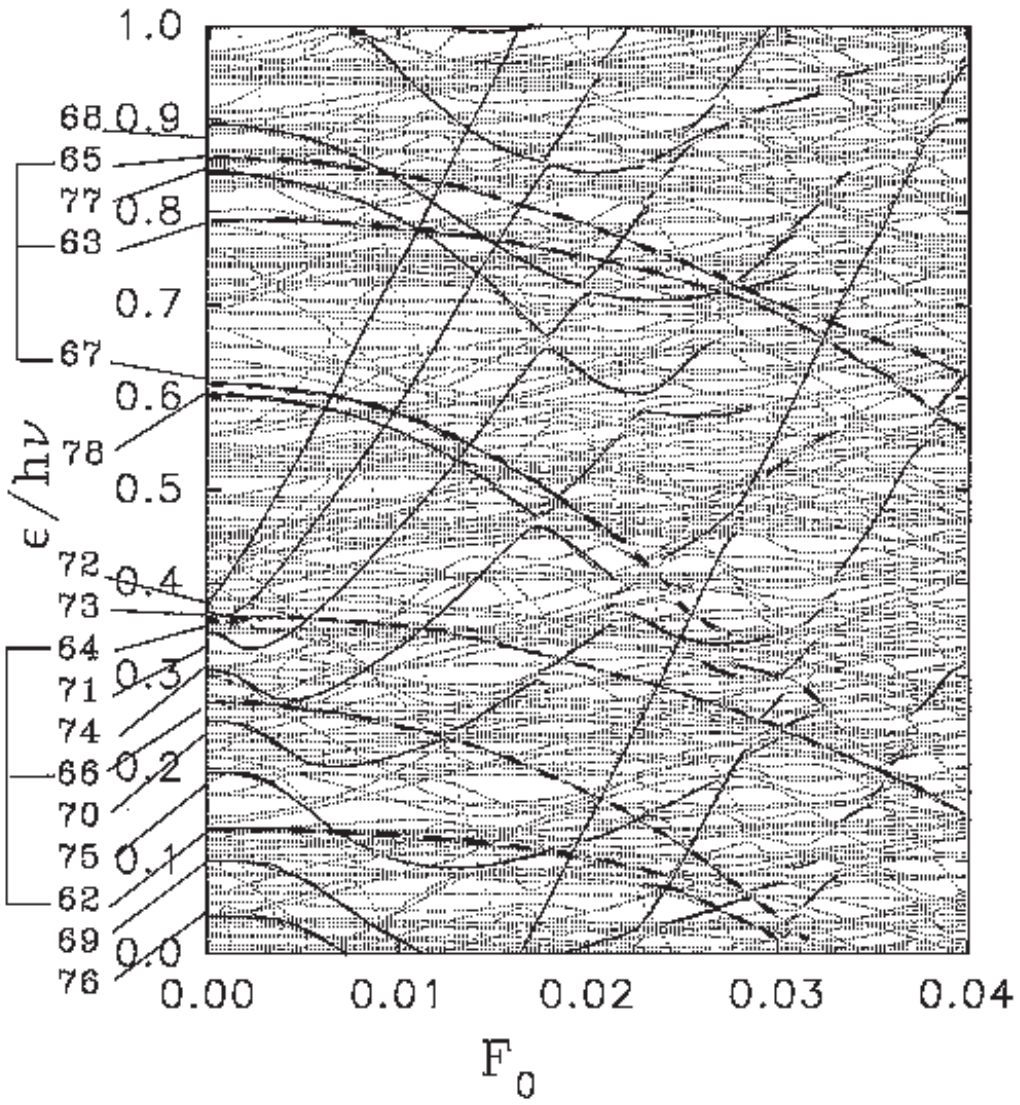

FIG. 13: a) The evolution of the projections of the wavefunction on the instantaneous Floquet states at every period of the rising edge of the microwave pulse. The parameters are: $\omega_0' = 0.685$, $F_0^{max} = 0.04$, $F_{0S} = 0.02777$, $T = 116$ microwave periods and $n_0 = 65$. The two states making up most of the probability are $n = n_0 = 65$ (full line) and $n = 63$ (dashed line). b) Quasienergy curves for the rescaled (to $n_0 = 65$) parameters $\omega_0' = 0.685$ and $F_{0S} = 0.02777$; the horizontal scale is the rescaled microwave field strength. The curves of the levels belonging to the $\omega_0' = 1/1$ nonlinear quantum resonance are marked as full lines; the two groupings of those belonging to the $\omega_0' = 2/3$ nonlinear quantum resonance as dashed lines.

.

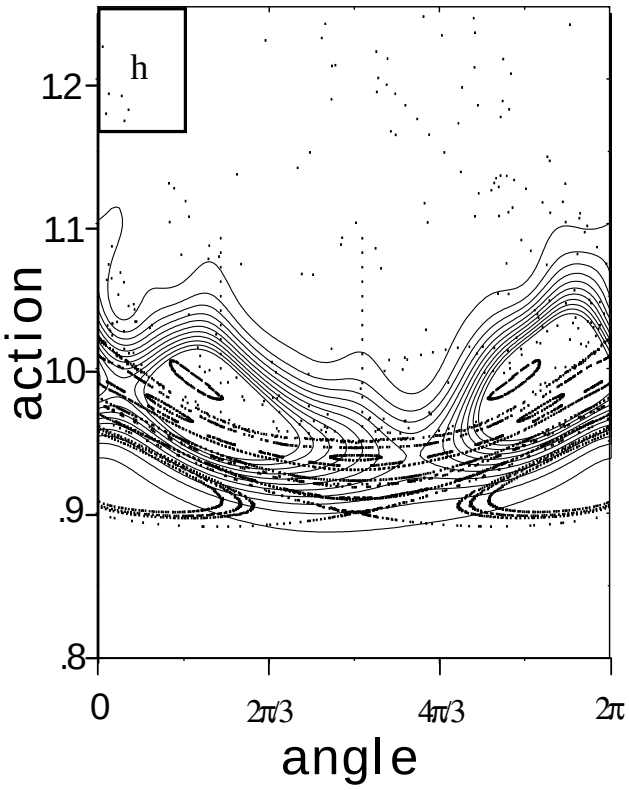
h
1.2
1.1
1.0
.9
.8
action
0
2π/3
4π/3
2π
angle

.

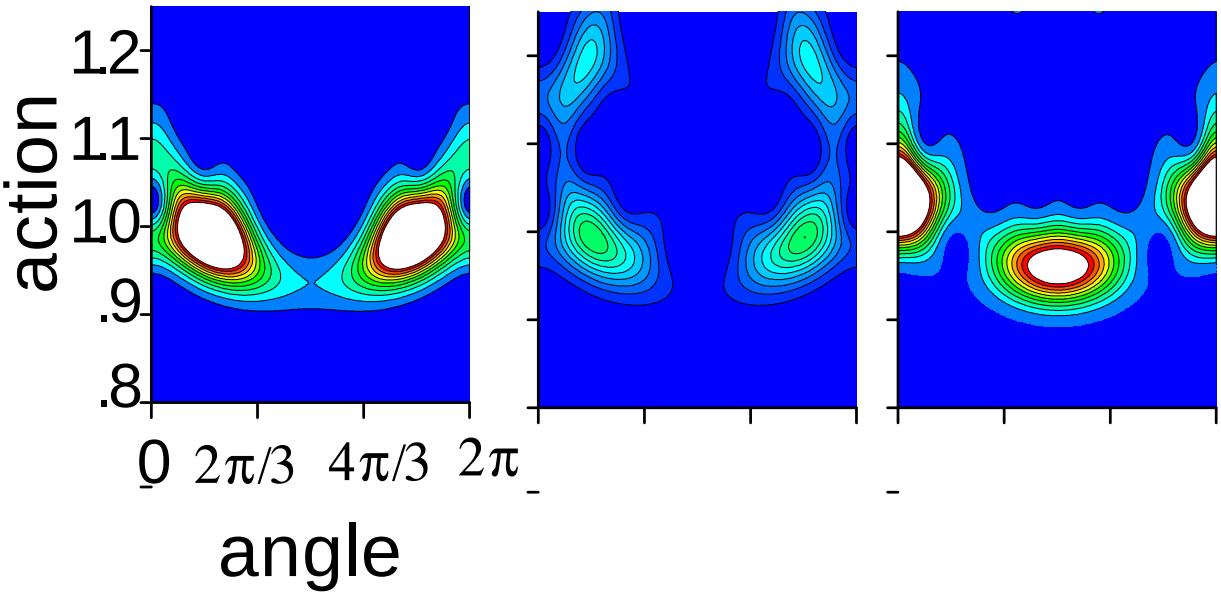

FIG. 14: a) Husimi function of the quantum wavefunction at the peak of the pulse superimposed over the classical surface of section at the same time. The parameters are $\omega_0' = 0.675$, $F_0^{max} = 0.04$, $F_{0S} = 0.02777$, $T = 116$ microwave periods and $n_0 = 65$. b) Husimi functions of the three eigenstates on which the above instantaneous wavefunction has the highest projections: in the order two states supported by the two islands of the $\omega_0' = 2/3$ classical resonance zone (62.3% and 15.7% respectively) and a state supported by the chaotic separatrix zone (12.7%).

.

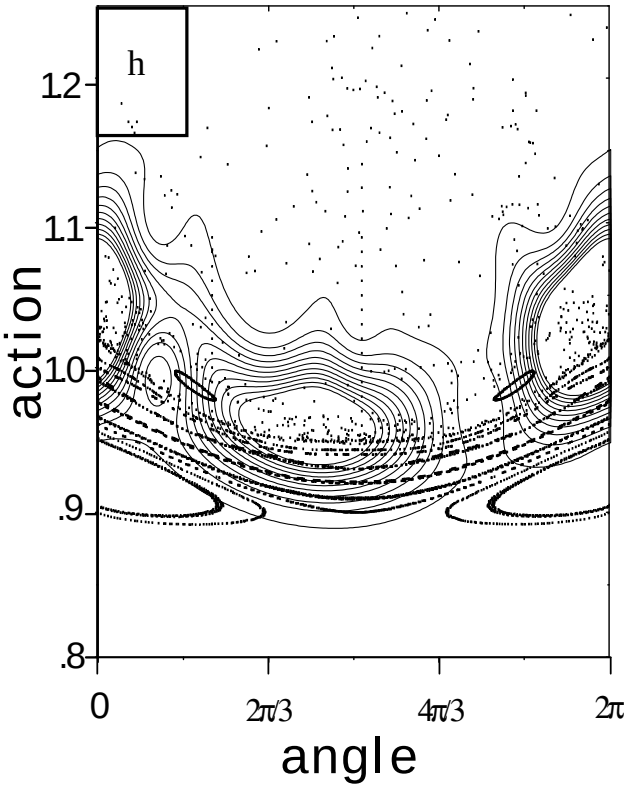
h
1.2
1.1
1.0
.9
.8
action
0
2π/3
4π/3
2π
angle

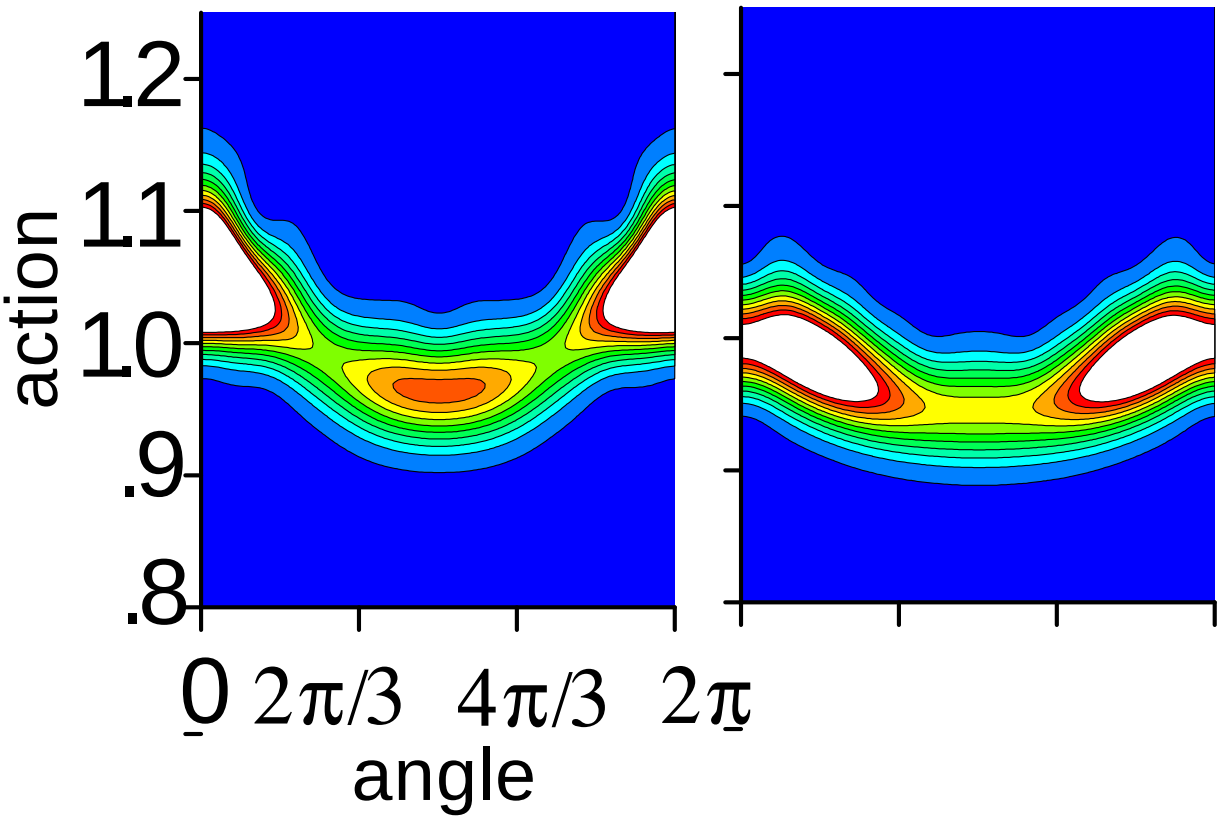

FIG. 15: a) Husimi function of the quantum wavefunction at the peak of the pulse superimposed over the classical surface of section at the same time. The parameters are $\omega_0' = 0.685$, $F_0^{max} = 0.04$, $F_{0S} = 0.02777$, $T = 116$ microwave periods and $n_0 = 65$. b) Husimi functions of the two eigenstates on which the above instantaneous wavefunction has the highest projections: in the order a state mostly localized around the unstable fixed point of the $\omega_0' = 1/1$ classical resonance zone (61.6%) and a state mostly supported by the two islands of the $\omega_0' = 2/3$ classical resonance zone (19.3%).

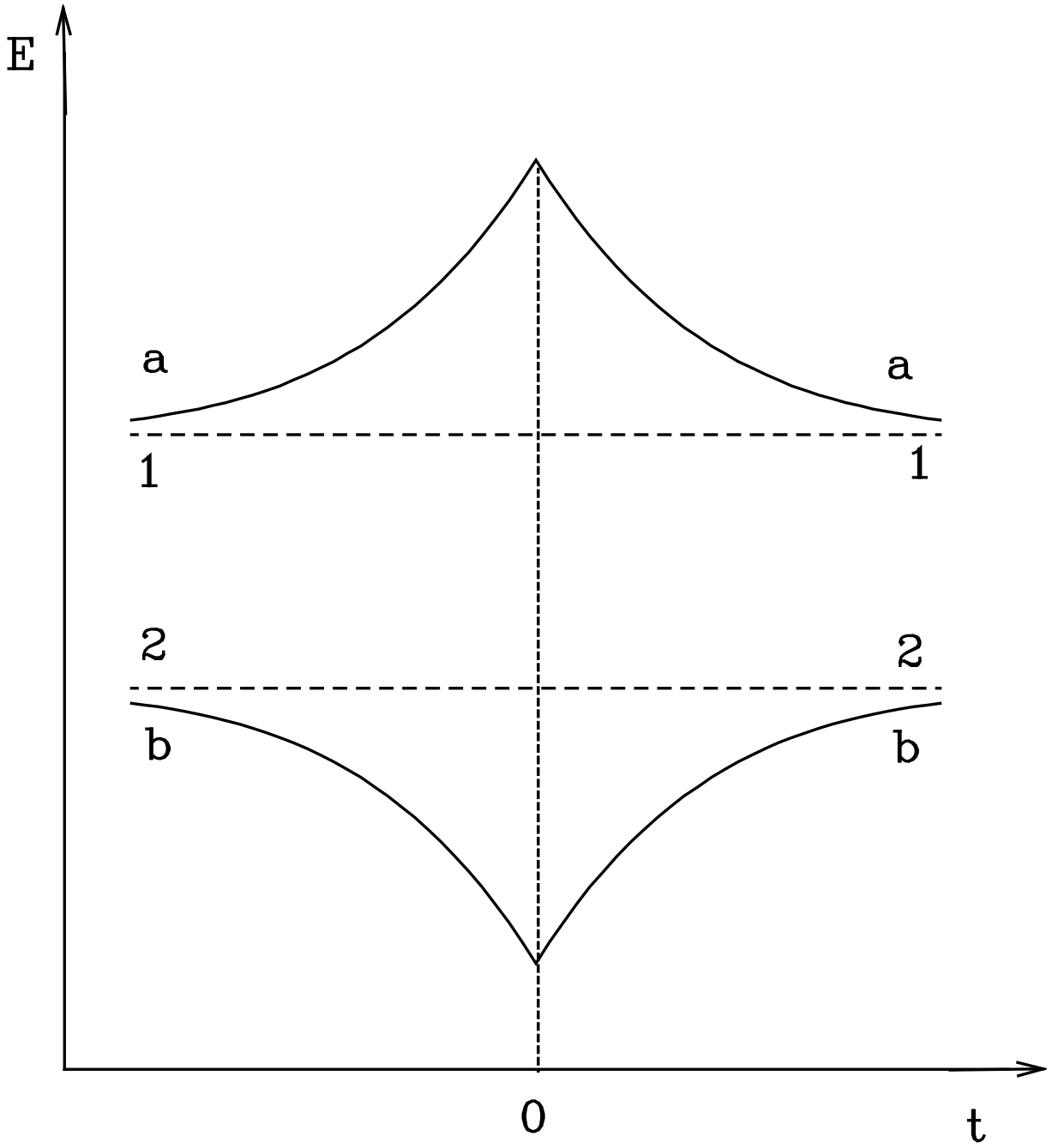

FIG. 16: Behaviour of the adiabatic (full lines) and diabatic (dashed lines) levels in the Demkov model as a function of time; the peak of the pulse is reached at $t = 0$. (From Ref. [22])

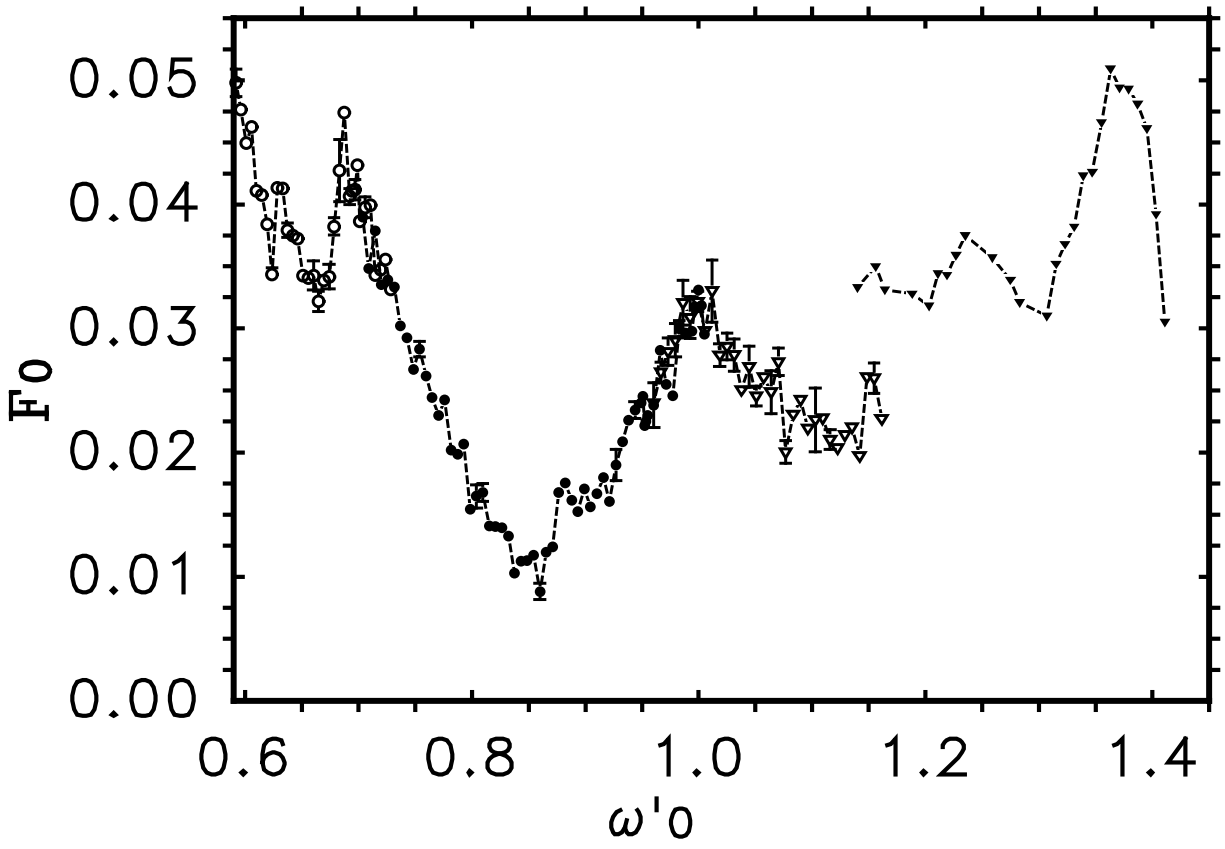
0.05
0.04
0.03
0.02
0.01
0.00
F0
0.6
0.8
1.0
1.2
1.4
ω'0

.

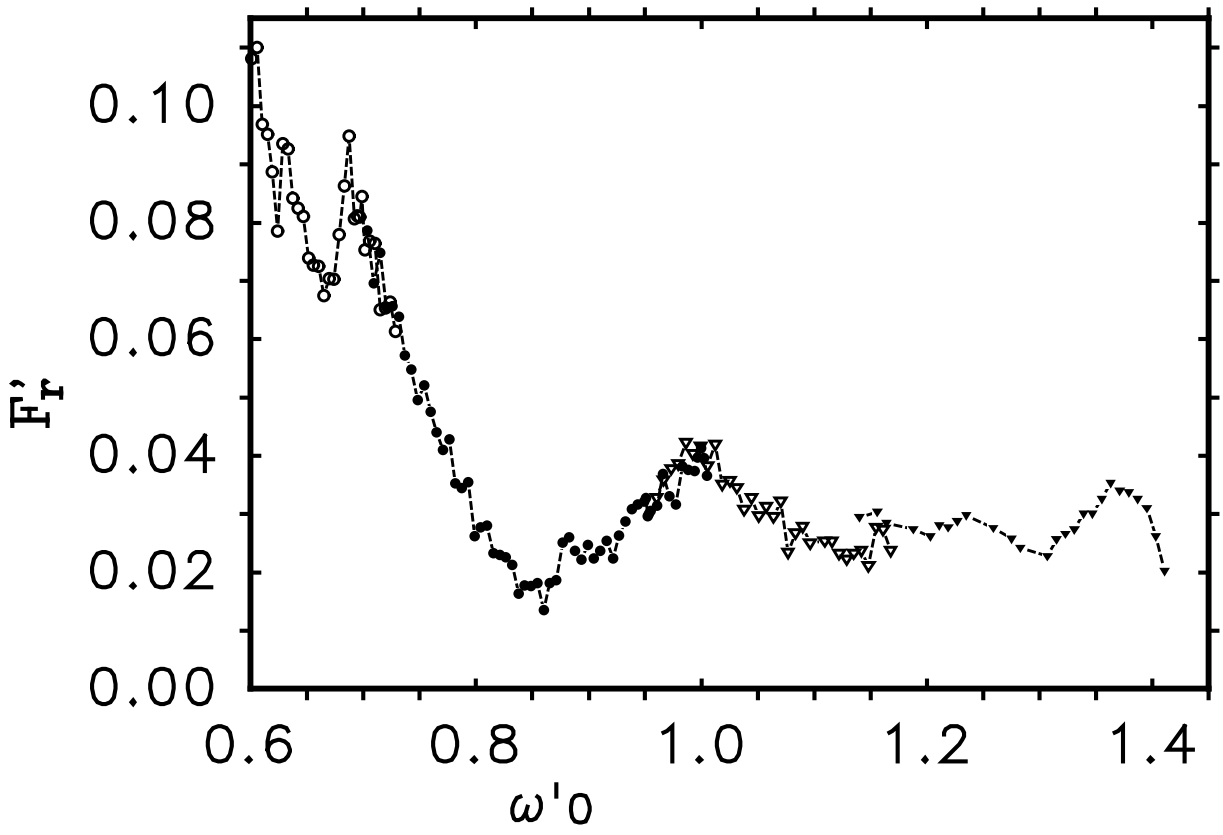

FIG. 17: Peak microwave field for 10% ionization probability a) rescaled to n_0 and b) rescaled to the central action of the principal primary resonance and corrected for the static field, both versus rescaled frequency ω_0': experimental results from Pittsburgh. circles: $n_0 = 65$, $F_S = 8\ \ V/cm$; dots: $n_0 = 69$, $F_S = 8\ \ V/cm$; empty triangles: $n_0 = 72$, $F_S = 8\ \ V/cm$; triangles: $n_0 = 80$, $F_S = 1\ \ V/cm$. The sharp break between the $F_S = 8\ \ V/cm$ data and the $F_S = 1\ \ V/cm$ ones in a) has disappeared with the new choice of rescaling. (From Ref. [22])